Retinal Ganglion Cells: A Functional Interpretation of Dendritic Morphology

C. Koch; T. Poggio; V. Torres

Stable URL:

http://links.jstor.org/sici?sici=0080-4622%2819820727%29298%3A1090%3C227%3ARGCAFI%3E2.0.CO%3B2-7

Philosophical Transactions of the Royal Society of London. Series B, Biological Sciences is currently published by The Royal Society.

RETINAL GANGLION CELLS:
A FUNCTIONAL INTERPRETATION OF
DENDRITIC MORPHOLOGY

By C. KOCH†, T. POGGIO†‡ AND V. TORRE§

† *Max-Planck-Institut für biologische Kybernetik,*
Spemannstrasse 38, *D* 7400 *Tübingen, F.R.G.*
§ *Università di Genova, Istituto di Fisica,*
Genova, Italy

CONTENTS

‡ Present address: M.I.T. Department of Psychology and Artificial Intelligence Laboratory, Cambridge, Massachusetts 02139, U.S.A.

The electrical properties of the different anatomical types of retinal ganglion cells in the cat were calculated on the basis of passive cable theory from measurements made on histological material. Standard values for the electrical parameters were assumed ($R_i = 70\ \Omega$ cm, $C_m = 2\ \mu$F cm^{-2}, $R_m = 2500\ \Omega$ cm^2). We conclude that these neurons need not be equipotential despite their small dimensions, mainly because of their extensive branching.

The interactions between excitation and inhibition when the inhibitory battery is near the resting potential can be strongly nonlinear in these cells. To characterize the different types of ganglion cells in terms of this property we introduce F, the factor by which the soma depolarization induced by a given excitatory input is reduced by inhibition. In this framework we analyse some of the integrative properties of an arbitrary passive dendritic tree and we then derive the functional properties that are characteristic for the various types of ganglion cells.

Our main results are:

(i) Nonlinear saturation at the synapses may be made effectively smaller by spreading the same (conductance) input among several subunits on the dendritic field. Subunits are defined as regions of the dendritic field that are somewhat isolated from each other and roughly equipotential within.

(ii) Shunting inhibition can specifically veto an excitatory input, if it is located on the direct path to the soma. The F values can then be very high even when the excitatory inputs are much larger than the inhibitory, as long as the absolute value of inhibition is not too small. Inhibition more distal than excitation is much less effective.

(iii) Specific branching patterns coupled with suitable distribution of synapses are potentially able to support complex information processing operations on the incoming excitatory and inhibitory signals.

The quantitative analysis of the morphology of cat retinal ganglion cells leads to the following specific conclusions:

(i) None of the cells examined satisfies Rall's equivalent cylinder condition. The dendritic tree cannot be satisfactorily approximated by a non-tapering cylinder.

(ii) Under the assumption of a passive membrane, the dendritic architecture of the different types of retinal ganglion cells reflects characteristically different electrical properties, which are likely to be relevant for their physiological function and their information processing role:

(a) α cells have spatially inhomogeneous electrical properties, with many subunits. Within each subunit nonlinear effects may take place; between subunits good linear summation is expected. F values are relatively low.

(b) β cells at small eccentricities have rather homogeneous electrical properties. Even distal inputs are weighted rather uniformly. Electrical inhomogeneities of the α type appear for β cells at larger eccentricities. F values are low.

(c) γ-like cells have few subunits, each with high input resistance underlying non-linear saturation effects possibly related to a sluggish character. F values are high: inhibition of the shunting type can interact in a strongly nonlinear way with excitatory conductance inputs.

(d) δ-like cells show many subunits with a high input resistance, covering well the dendritic area. Within each subunit inhibition on the direct path to the soma can specifically veto a more distal excitation. It is conjectured that such a synaptic organization superimposed on the δ cell morphology underlies directional selectivity to motion.

(iii) Most of our data refer to steady-state properties. They probably apply, however, to all light evoked signals, since transient inputs with time to peak of 30 ms or more can be treated in terms of steady-state properties of the ganglion cells studied.

(iv) All our results are affected only slightly by varying the parameter values within reasonable ranges. If, however, the membrane resistance were very high, all ganglion cells would approach equipotentiality. For $R_m = 8000 \ \Omega \ cm^2$ subunits essentially disappear in all types of ganglion cells (for steady state inputs). Our results concerning nonlinear interaction of excitation and inhibition (F values) would, however, remain valid even for much larger values of R_m and for any value of R_i larger than 30–50 Ω cm. The critical requirement is that peak inhibitory conductance changes must be sufficiently large (around 5×10^{-8} S) with an equilibrium potential close to the resting potential. Underestimation of the diameters of the dendritic branches may affect these conclusions (F could be significantly lower).

1. INTRODUCTION

1.1. Relevance of dendritic branching

A common way of assessing whether the dendritic tree of a neuron is equipotential is to compare its average length (l) with its estimated electrotonic space constant (λ). If λ is greater than l it is then concluded that the soma dendritic complex is a reasonably equipotential structure. With standard values for R_m (the membrane resistance; $R_m = 2500 \ \Omega \ cm^2$) and R_i (the intracellular resistivity; $R_i = 70 \ \Omega \ cm$), $\lambda = 298.8 \ \mu m$ $(d)^{\frac{1}{2}}$, where d is the dimensionless dendritic diameter in micrometres. Since $d = 1 \ \mu m$ gives $\lambda = 298.8 \ \mu m$ and $d = 4 \ \mu m$ gives $\lambda = 597.6 \ \mu m$, only neurons with dendritic trees larger than 300–500 μm could show non-uniform electrical properties. Since the main dendritic branches of retinal neurons have diameters between 1 and 4 μm, most retinal cells should then be considered electrically equipotential, with the possible exception of the long processes of horizontal cells (see, for example, Weiler & Zettler 1979) and possibly some large cells in the innerplexiform layer (like peripheral α ganglion cells). The argument, if correct, would seem to have the strong implication that the dendritic morphology of most retinal cells is of no consequence for the electrical and functional properties of the cells, apart from merely reflecting the spatial extent of connections.

The above reasoning is strictly correct for a cylindrical cable. In branched structures, even those satisfying the equivalent cylinder condition, the previous argument can be totally wrong, however, as Rall (1977; see also Rall & Rinzel 1973) has clearly pointed out. When a pulse of

current is injected into one of the terminal tips the attenuation between the voltage observed in the tip and the soma can be orders of magnitude higher than the voltage attenuation between the soma and the tip, when the same input is injected into the soma. This asymmetry depends substantially on the number of branchings and disappears for zero branching. Thus, the previous argument is correct for the attenuation from the soma and is otherwise wrong. As a consequence dendritic branching is an important determinant of the passive electrical properties even of small neurons. It therefore seems highly likely that the branching pattern and shape of the dendritic tree have a special significance for the passive integration of incoming signals. The interpretation of dendritic architecture for the processing function of cells becomes a challenging problem and is the theme of this paper.

The dendritic tree of ganglion cells in the vertebrate retina offers a rare opportunity for a quantitative approach to this issue, since it is spread out as an almost two dimensional branched pattern. The possibility of relating the form of the ganglion cells to their function was opened up for the first time by the morphological classification of Boycott & Wässle (1974). They separated cat retinal ganglion cells into three distinct classes, α, β, γ and tentatively a fourth class, δ, mainly on the basis of the highly specific branching pattern of the dendrites. Increasingly, physiological and other evidence suggests that the morphological α, β and γ (plus δ) classes are related to the physiological Y, X and W types, respectively (see: Levick 1975; Lennie 1980; Peichl & Wässle 1981).

In this paper we develop some simple theoretical tools for describing the main integrative properties of an arbitrary dendritic tree with passive membrane properties. The key notions are represented by the concept of a 'subunit', which illustrates the electrical inhomogeneities of a cell, and by the *direct path* condition, which is the main prerequisite for shunting inhibition to veto effectively and specifically an excitatory input. We then derive from the morphology of the different types of cat retinal ganglion cells the electrical properties to be expected on the basis of classical cable theory. The α, β, γ and δ ganglion cells turn out to have different passive electrical properties which can be connected to their characteristic function. In particular, specific branching patterns with a suitable distribution of synapses may underly complex nonlinear operations.

In most of our calculations we used $R_m = 2500 \ \Omega \ cm^2$ for the membrane resistance, $R_i = 70 \ \Omega \ cm$ for the intracellular resistivity, $C_m = 2 \ \mu F \ cm^{-2}$ for the membrane capacitance. These values can be regarded as normal, at least for other preparations (see, for example, Rall 1977; Barrett 1975). We checked, however, all our calculations for values of R_m up to $8000 \ \Omega \ cm^2$ or higher. It is important to stress that we have assumed that the dendritic membrane is passive, i.e. no local response or dendritic spike occurs. The effect of active membrane properties in the dendrites will be studied elsewhere.

1.2. *Organization of the paper*

The paper is divided in three main parts. The first part describes the methods used in the course of our analysis, starting with the computer program that computes the main passive electrical properties of the various cells from their quantitative histological data (§2.1). The notion of a subunit of a dendritic field is introduced in §2.2 as a way of visualizing spatial inhomogeneity of the electrical properties of a cell. In §2.3.1 it is shown that postsynaptic saturation, i.e. nonlinear summation of synaptic inputs, can be reduced by distributing the total (conductance) input among different subunits. The interaction between excitatory and

inhibitory synapses is discussed in §2.3.2, especially for shunting inhibition. The *direct path* condition plays here the central role: inhibition of the shunting type can effectively veto the somatic depolarization induced by an excitatory input only if it is located on the direct path from the location of excitation to the soma. The rest of the paper describes the application of these methods and ideas to retinal ganglion cells. The second part characterizes the different morphological classes in terms of passive cable properties (§3.1) and nonlinear interactions of synaptic conductance inputs (§3.2). The role of parameter values (membrane resistance, intracellular resistivity and membrane capacitance) in our calculations is examined in §3.3. The functional implications of these results are discussed in the third part of the paper. Physiological properties of the various classes of ganglion cells are interpreted in the light of their electrical properties (§4.1). In §4.2 we suggest that a γ-like and a δ-like morphology may underly characteristic information processing operations. A discussion of directional selectivity leads to a specific conjecture about its morphological basis in the cat retina (§4.3).

2. METHODS

2.1. *Histological data and computational methods*

Our data are taken from two of the Golgi–Cox stained whole mount retinae of one adult cat described in Boycott & Wässle (1974; see also Boycott *et al.* 1978). Each analysed cell was traced at ×400 to ×1000 magnification with use of a Zeiss drawing apparatus. The branching structure, the length and the diameter of each dendritic segment were determined from these anatomical measurements. The dendritic tree was approximated in terms of short segments, each being equivalent to a cylinder. Each dendritic segment for which the diameter did not change by more than 0.2 μm was described as an equivalent cylinder of length l and (average) diameter d. The dendritic tree can be considered in all cases as an essentially two dimensional structure and is so treated here. Even when different branches of the same cell overlap (see figures 2 and 6), the depth difference is about 3 μm and seldom larger. The only significant deviations from planarity arise, especially for cells near the central area, around the soma which lies about 15–30 μm deeper than the dendritic tree. We checked the effect of neglecting this three dimensional effect in our calculations. All values given in the tables remain essentially unchanged apart from some K_{is} values (see later in this section); the upper bound of their error, however, is below 4 % and usually much less for most cells and locations.

We also measured the three dimensional structure of the soma by focusing at various depths and tracing its contours. The soma was described as a series of appropriate cylindrical slabs. Although their diameters are larger than their lengths, one dimensional cable theory is still an excellent approximation as we confirmed in some model cases. The smallest measurable diameter was estimated to be about 0.2 μm, which is approximately the resolution of the Zeiss microscope. Lengths and diameters were corrected for shrinkage, by multiplying their values by 1.3 (see Peichl & Wässle 1979).

Branching structure, lengths and diameters were coded into a list that served as input to the program NEURON, written in Pascal (Koch 1982), which computes the characteristic electrical properties of the cell. In addition, we computed the total membrane area of the soma (S) and of the dendrites (D) and the total number of terminals (n). The electrical quantities used are the electrotonic distance of each terminal from the soma (L), the transfer resistances K_{ij} the voltage (A_V) and the current (A_I) attenuation factors. We turn now to the definitions of these electrical quantities.

Electrotonic distance

The electrotonic distance L is defined as

$$L = \int_{soma}^{tip} dx/\lambda(x),$$ (2.1)

where

$$\lambda(x) = \left[\frac{R_m}{R_i}\frac{d(x)}{4}\right]^{\frac{1}{2}},$$ (2.2)

where $d(x)$ is the diameter of the cylindrical segment at the linear distance x from the soma.

Transfer resistances

The main electrical quantity computed by NEURON, under the assumption of sealed end terminations, is the complex transfer resistance $\tilde{K}_{ij}(\omega)$.

If a current I_j is injected at location j the voltage at location i is

$$V_i(t) = I_j(t) * K_{ij}(t),$$ (2.3)

where $*$ indicates convolution. The Green function $K_{ij}(t)$, i.e. the inverse Fourier transform of $\tilde{K}_{ij}(\omega)$, is the voltage response at location i when a delta pulse of current is injected at location j. The d.c. value $\tilde{K}_{ij}(0)$ is the transfer resistance between i and j for d.c. inputs in j. If the two locations coincide $(i = j)$ one obtains the familiar input resistance at that location. The complex functions $\tilde{K}_{ij}(\omega)$ for various locations i, j completely characterize the (linear) electrical properties of a branched passive cable. Two general properties of the $\tilde{K}_{ij}(\omega)$ for dendritic trees (without loops) are especially useful (see: Poggio & Torre 1982; Koch 1982):

$$\tilde{K}_{ij}(\omega) = \tilde{K}_{ji}(\omega)$$

and

$$\tilde{K}_{ij}(\omega) = \tilde{K}_{il}(\omega)\tilde{K}_{lj}(\omega)/\tilde{K}_{ll}(\omega)$$

for l on the direct path from i to j.

The algorithm implemented by the program is an extension of the Butz & Cowan (1974) scheme. The accuracy of the program has been checked by comparing the numerical solutions with analytical solutions that are available for unbranched cylinders. Further comparisons were made for branched trees with another algorithm which will be described elsewhere (Poggio & Torre 1982).

Attenuation and charge factors

It is useful to introduce two types of attenuation factors: first, the voltage attenuation factor A_V^{ij}, defined as

$$A_V^{ij} = V_i/V_j.$$ (2.4)

This is the ratio between the voltage at location i and location j when an arbitrary input (current injection or conductance change) occurs at i. It is easy to see that

$$\tilde{A}_V^{ij}(\omega) = \tilde{K}_{ii}(\omega)/\tilde{K}_{ij}(\omega).$$ (2.5)

In what follows, we will consider only the attenuation factor between the input location i and the soma, i.e.

$$\tilde{A}_V^{i}(\omega) = \tilde{K}_{ii}(\omega)/\tilde{K}_{is}(\omega).$$ (2.6)

In a similar way we introduce the current attenuation factor A_I, defined as

$$A_I^i = I_i/I_s,\tag{2.7}$$

i.e. the ratio between the input current at location i and the current reaching the soma. Analogously

$$\tilde{A}_I^i(\omega) = \tilde{K}_{ss}(\omega)/\tilde{K}_{is}(\omega).\tag{2.8}$$

Since $\tilde{I}_i(0) = \int_{-\infty}^{+\infty} I_i(t)\,dt$, $\tilde{I}_i(0)$ is the total injected charge in location i. Thus $Q = 1/\tilde{A}_I(0)$ is the charge factor, i.e. the fraction of the injected charge reaching the soma (Barrett & Crill 1974b; Rinzel & Rall 1974). It is important to notice that Q is independent of the time course of the input current.

In this paper we will mainly consider steady state inputs and, correspondingly, the quantities $\tilde{K}_{ij}(0)$, which for simplicity will be denoted in the following as K_{ij}. For transient inputs of a given time course $I(t)$ (for instance $I(t)$ can be taken as $t\,e^{-t/t_{peak}}$) it is convenient to define a single real number that we shall call *effective impedance* as

$$K_{ij}^{eff} = V_i^{peak}/I_j^{peak}.$$

K_{ij}^{eff} depends in general on the time course of the input current $I(t)$ (but not on its amplitude). It is essentially independent of the time course for all inputs that are either much faster or much slower than the Green function $K_{ij}(t)$. Even when these conditions are not satisfied, and therefore an effective resistance cannot be uniquely determined, K_{ij}^{eff} gives a quantitative measure of the transfer properties of the neuron for given transient inputs.

2.2. *Defining a subunit*

If a neuron is not equipotential, its electrical properties, i.e. input and transfer resistances, attenuations etc., are not uniform in the sense that they strongly depend on input–output location. This being so, it is natural to try to divide the dendritic tree into electrically homogeneous regions, each one being rather isolated from the other and rather equipotential within. We wish to propose the term *subunit* for such regions of the dendritic tree.†

The notion of a subunit does not apply to neurons that receive a massive synaptic stimulation over the whole dendritic tree, since these are then essentially equipotential. Our approach is mainly concerned with neurons with specific and localized synaptic inputs.

We define a subunit as a region of the dendritic tree where

(i) the attenuation within is not larger than a value a, i.e.

$$K_{ii}/K_{ij} \leqslant a \quad (a > 1)\tag{2.9a}$$

for all locations i, j that belong to the subunit, and

(ii) the attenuation between each point i of the subunit and the soma is larger than a value b, i.e.

$$K_{ii}/K_{is} > b \quad (b > 1).\tag{2.9b}$$

A subunit is thus characterized in terms of the two quantities a and b. As a approaches 1, the subunit becomes smaller and more homogeneous. As b increases, the subunit becomes

† The term subunit has already been used with a different meaning, by Barlow & Levick (1965) and by Hochstein & Shapley (1976b).

more and more decoupled from the soma and, again, smaller and smaller. Since, for the purpose of the work discussed here decoupling of the subunit from the soma is more critical than its electrical homogeneity, we have used a less rigorous definition instead of equation (2.9b), namely

$$K_{ij}/K_{is} > c \quad (c > 1) \tag{2.9c}$$

for every i and j belonging to the subunit.

This definition (equation (2.9c)), together with the additional requirement that the resulting subunits should not overlap, allows us to partition a dendritic tree into regions that are decoupled and almost equipotential. The maximal set of non-overlapping subunits thus defined is clearly not unique. Since the solutions of the cable equation are continuous along branches, it is formally impossible to define subunits as disjoint regions with distinct boundaries. In practice, our definition of a subunit was used in the following way (see figures 2–6). An initial distal dendritic tip i was arbitrarily chosen and the set of locations j satisfying equation (2.9c) was determined (with $c = 4$). A nearby distal tip not contained in the previous subunit was then considered in like manner, and so on around the dendritic tree.

The concept of a subunit, as we have introduced it, is clearly empirical and cannot be cast into a rigid form in terms of electrical properties alone. It is mainly of value as a way of visualizing directly the spatial inhomogeneities of the electrical properties of the cells and its importance should not be overemphasized. The dimensions and the number of the subunits, for instance, are only indicative. They depend on the parameter c which is rather arbitrarily chosen. We have given c the value 4; $c = 3$ yields roughly the same picture with somewhat larger subunits (see figure 4).

2.3. Synaptic interactions

Synaptic inputs consist of conductance changes $g_i(t)$ to ionic species with equilibrium potential E. The resulting current $I_i(t)$ in location i is, in general, not proportional to $g_i(t)$ since

$$I_i(t) = g_i(t)\,[E - V_i(t)], \tag{2.10}$$

where, of course, $V_i(t)$ depends on $I_i(t)$ and possibly on other inputs. Different kinds of interactions occur when there are several similar synapses (either excitatory or inhibitory) or when there are both excitatory and inhibitory synapses.

2.3.1. Nonlinear addition for synaptic inputs of one type

Let us consider synapses that modulate the conductance g to a particular ion with equilibrium potential E. For the sake of simplicity let us suppose that the synapse is excitatory, i.e. $E > V_{\text{rest}} = 0$. For a single synapse at location i, the potential V_i is given, for steady-state inputs,

$$V_i = K_{ii} I_i. \tag{2.11}$$

Equations (2.11) and (2.10) give

$$V_i = K_{ii} g E / (1 + K_{ii} g), \tag{2.12}$$

yielding for the voltage at the soma

$$V_s = V_i K_{is} / K_{ii},$$

i.e.

$$V_s = K_{is} g E / (1 + K_{ii} g). \tag{2.13}$$

From equation (2.13) we see that, for small values of g, V_s is proportional to $K_{\mathrm{is}}gE$, and, for very large values of g, $V_\mathrm{s} = K_{is}E/K_{ii}$. The value $K_{is}E/K_{ii}$ is the maximal depolarization produced in the soma by a single synapse at location i. This is the well known effect of non-linear addition (or synaptic saturation).

We will show now that for a neuron that has N identical subunits, the degree of synaptic saturation can be greatly reduced if the same total conductance change is distributed among the N subunits. We assume that each subunit has the same input impedance K_{ii}, the same transfer resistance to the soma K_{is}, and the same reciprocal transfer resistance K_{ij}, where i and j are located in different subunits.

The synaptic current in each subunit is then

$$I_i = (g/N)(E-V_i),\tag{2.14}$$

while V_i takes the form

$$V_i = K_{ii}I_i + (N-1)K_{ij}I_j.\tag{2.15}$$

Since all synapses are assumed to be similar we obtain

$$V_i = gK_{ii}^{av}E/(1+gK_{ii}^{av})\tag{2.16}$$

with
$$K_{ii}^{av} = [K_{ii}+(N-1)K_{ij}]/N\tag{2.17}$$

and at the soma

$$V_\mathrm{s} = NK_{is}I_i$$

i.e.
$$V_\mathrm{s} = gK_{is}(E-V_i)$$

or
$$V_\mathrm{s} = gK_{is}E/(1+gK_{ii}^{av}).\tag{2.18}$$

For small values of g, V_s is still proportional to $gK_{is}E$: the maximal value of V_s is now, however, $K_{is}E/K_{ii}^{av}$, and, since $K_{ii}^{av} < K_{ii}$, the maximal voltage depolarization induced in the soma is increased by the factor G:

$$G = K_{ii}/K_{ii}^{av}.\tag{2.19}$$

Thus, saturation is effectively reduced. Therefore, in neurons with a large number of subunits, the maximal evoked somatic depolarization can be greatly increased by distributing the same conductance change among the various subunits (compare Barrett & Crill 1974b).

2.3.2. Interactions between excitatory and inhibitory inputs: the direct path condition

The combination of an excitatory and an inhibitory conductance input may give rise to strong nonlinear interactions (Poggio & Torre 1978; see also Barrett 1975; Redman 1976). Let us consider an excitatory synapse modulating the conductance g_e to an ionic species with equilibrium potential $E_e > V_{\mathrm{rest}} = 0$ in location e, and an inhibitory synapse modulating the conductance g_i to an ionic species with equilibrium potential $E_i \leqslant V_{\mathrm{rest}} = 0$ in location i. When the conductance g_e and g_i are steady state inputs, the associated equations become simply

$$V_\mathrm{s} = g_e(E_e-V_e)K_{es} + g_i(E_i-V_i)K_{is},$$
$$V_e = g_e(E_e-V_e)K_{ee} + g_i(E_i-V_i)K_{ie},$$
$$V_i = g_e(E_e-V_e)K_{ei} + g_i(E_i-V_i)K_{ii}\tag{2.20}$$

and the voltage in the soma can be calculated as

$$V_\mathrm{s} = \frac{g_eE_e(K_{es}+g_iK_e^+) + g_iE_i(K_{is}+g_eK_i^+)}{1+g_eK_{ee}+g_iK_{ii}+g_eg_iK^*}\tag{2.21}$$

with
$$K_i^+ = K_{is}K_{ee} - K_{es}K_{ei},$$
$$K_e^+ = K_{es}K_{ii} - K_{is}K_{ie},$$
$$K^* = K_{ee}K_{ii} - K_{ie}K_{ie}. \qquad (2.22)$$

From equation (2.21) it is possible to prove that *for any arbitrary value of* g_e *and* g_i *the location where inhibition is maximally effective is always on the direct path from the location of the excitatory synapse to the soma.* The proof will be given elsewhere (Poggio & Torre 1982; Koch 1982).

We now list a series of useful properties, concerning the optimal location of inhibition (see also: Jack *et al.* 1975; Rall 1967, 1970), which are valid for d.c. conductance inputs in arbitrary dendritic trees.

(i) For small synaptic inputs, the most relevant parameter is the distance of the inhibitory synapse from the excitatory synapse. In this case it makes little difference whether the inhibition is behind the excitation or on the direct path to the soma. If the inhibition is of the shunting type ($E_i = 0$), the optimal location is at the site of excitation.

(ii) When the amplitude of the excitatory synaptic input increases, and the inhibitory conductance change remains unaltered, the optimal location of inhibition moves towards the soma along the direct path.

(iii) For very large excitatory inputs ($g_e \to \infty$) all inhibitory synapses located behind the excitatory synapse are completely ineffective.

(iv) For very large shunting inhibitory inputs ($E_i = 0$ and $g_i \to \infty$) all locations on the direct path from the excitatory synapse to the soma are equally effective.

All these properties are direct consequences of equation (2.21) and the fact that in dendritic trees there is only one direct path from any point to the soma. Property (i) has been obtained by using the additional property that the input resistance decreases when the location of inhibition moves from the tip towards the soma on the direct path.

From equation (2.21) it is clear that when $E_i = 0$ the effect of inhibitory synapses is evident only when the excitatory synapses are active. This is the well known phenomenon of 'shunting inhibition'. When E_i is well below V_{rest} (which we have assumed to be zero) the first contribution of the inhibitory synaptic conductance change to V is $g_i E_i K_{is}$. This contribution, which coincides with the linear component of the inhibition, is maximal for somatic inhibition. Therefore we have the general rule that, if E_i is much below the resting potential V_{rest}, synaptic inhibition will be more effective in or near the soma and inhibition and excitation will interact in an approximately linear way. When E_i is close to the resting potential somatic inhibition is less effective. Furthermore, the interaction between excitatory and inhibitory inputs becomes nonlinear. Whereas the inhibitory equilibrium potential in bipolar cells seems to be rather far from the resting potential, inhibition in some cells of the inner plexiform layer of the turtle retina is best approximated by a shunting inhibition (for amacrine cells see Marchiafava & Torre (1978); for ganglion cells Marchiafava (1979) and Baylor & Fettiplace (1979)). In this paper we will mainly consider shunting inhibition ($E_i = 0$), because this mechanism can underly more sophisticated interactions and may represent the predominant type of post-synaptic inhibition in some retinal ganglion cells.

As a measure of the effectiveness of shunting inhibition we introduce the ratio between the somatic depolarization for zero inhibition and that for non-zero inhibition. This factor F is, from equation (2.21),

$$F = \frac{g_e K_{es}}{1 + g_e K_{ee}} \frac{1 + g_e K_{ee} + g_i K_{ii} + g_e g_i K^*}{g_e K_{es} + g_e g_i K_e^+}, \qquad (2.23)$$

where $K_e^+ = 0$ for 'on path' locations of inhibition; $1/F$ indicates the relative decrease of the evoked voltage potential in the soma induced by the inhibitory conductance change g_i at location i. It also represents the ratio of the current reaching the soma when inhibition is active to the current due to excitation alone.
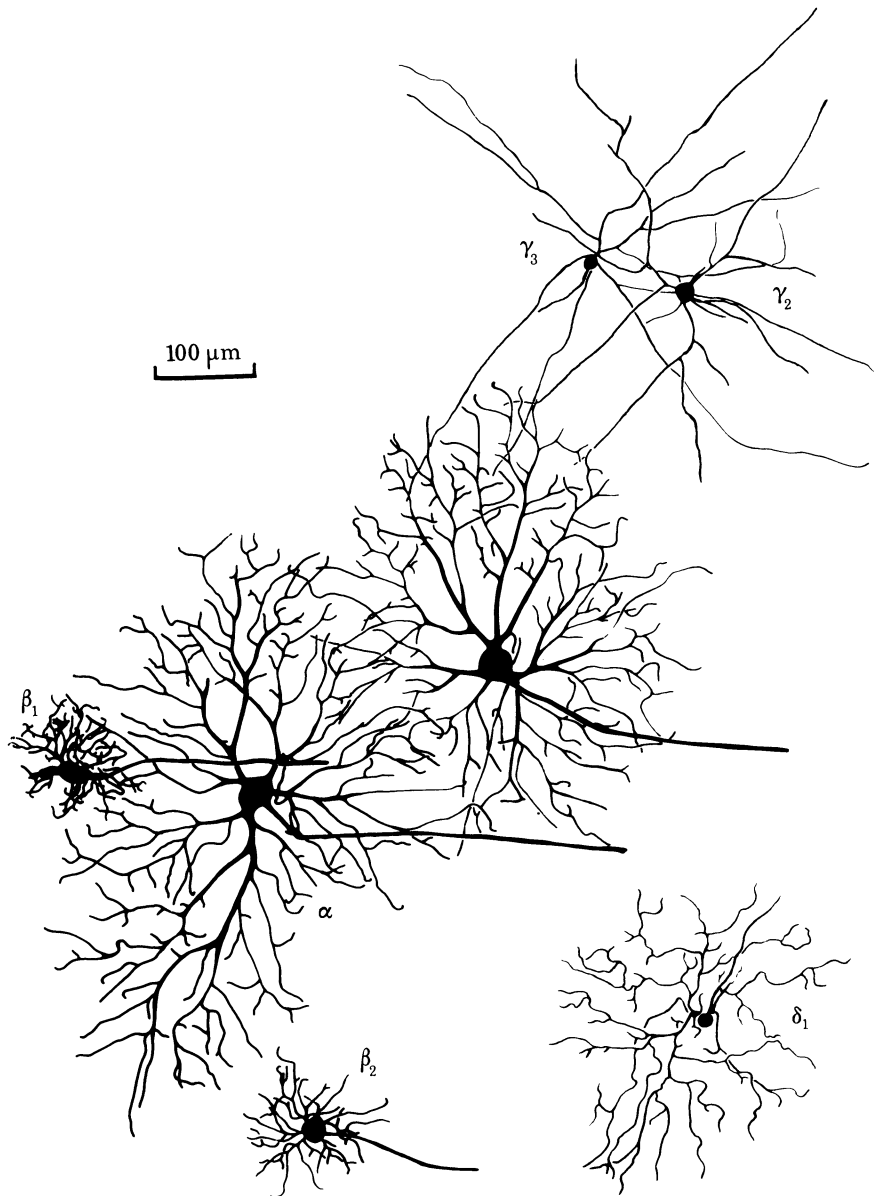
FIGURE 1. Six of the ganglion cells analysed are shown here. The δ cell (δ_1) is from the same retina and has about the same eccentricity (*ca.* 3 mm) but a different location. It has been pasted into the original drawing (Wässle *et al.* 1979; Golgi–Cox preparation). Each of the four types of cat retinal ganglion cells introduced by Boycott & Wässle (1974) is represented: two α cells, two β cells, two γ cells and one δ cell.

3. ANATOMICAL TYPES OF GANGLION CELLS: PASSIVE ELECTRICAL PROPERTIES

Six out of the nine retinal ganglion cells that we have analysed were located at about the same eccentricity (3 mm from the centre of the area centralis), in the same retina (figure 1). Figure 1 illustrates the typical forms of the various classes of ganglion cells, according to the Boycott & Wässle (1974) classification. The α cells have a relatively large, branched tree

with long distal dendrites and a large cell body. At the same eccentricity β cells are much smaller, have more branches per unit area, short distal dendrites and a medium sized cell body. Most γ cells have a small cell body and dendrites that are almost unbranched and thin. The δ cells may constitute a fourth morphological type of ganglion cells, although Boycott & Wässle had only seen a few of them. They are much more branched than γ cells but are similar to them in that their dendrites are thin and rather uniform even at branch points.

TABLE 1. CHARACTERISTIC PARAMETERS OF THE GANGLION CELLS EXAMINED

(The upper (lower) value of K_{ii} is the d.c. input impedance at the tips of first (second) centripetal branches averaged over all tips. Similarly, K_{is} is the d.c. transfer from tips to soma. Values for L, K_{ii} and K_{is} are means $\pm$ standard deviations. Standard parameter values are assumed: see text.)

cell	eccentricity mm	$D/10^{-4}$ cm² $S/10^{-4}$ cm²	n	d_t μm	L	$\dfrac{K_{ss}}{\text{MΩ}}$	$\dfrac{K_{ii}}{\text{MΩ}}$	$\dfrac{K_{is}}{\text{MΩ}}$	A_V	Q
α_{ON}	3	4.90/0.65	131	580	0.65 ± 0.18	5.6	102 ± 55 42 ± 23	4.0 ± 0.6 4.0 ± 0.5	25.6 10.5	0.71 0.71
$\beta_{1\ ON}$	3	0.69/0.29	48	157	0.22 ± 0.07	22.3	76 ± 39 43 ± 16	21.3 ± 0.4 21.4 ± 0.4	3.6 2.0	0.96 0.96
$\beta_{2\ ON}$	3	0.58/0.31	44	189	0.27 ± 0.09	31.0	130 ± 55 68 ± 23	29.1 ± 0.8 19.3 ± 0.8	4.5 2.3	0.94 0.95
$\beta_{3\ OFF}$	9	1.04/0.36	44	354	0.56 ± 0.17	19.9	200 ± 75 96 ± 43	15.8 ± 1.5 16.1 ± 1.5	12.7 6.0	0.79 0.81
$\beta_{4\ ON}$	9	1.60/0.48	58	420	0.64 ± 0.16	14.2	178 ± 58 94 ± 35	10.7 ± 0.9 10.9 ± 1.0	16.7 8.6	0.75 0.77
γ_2	3	0.63/0.24	16	471	0.82 ± 0.19	37.4	219 ± 139 113 ± 51	29.1 ± 4.6 29.8 ± 3.5	7.5 3.9	0.78 0.80
γ_3	3	1.17/0.08	12	642	1.06 ± 0.26	29.7	208 ± 87 83 ± 29	16.7 ± 4.0 20.1 ± 2.5	12.5 4.1	0.56 0.68
δ_1	3	1.17/0.09	65	386	0.63 ± 0.19	29.4	159 ± 63 105 ± 55	17.8 ± 3.2 18.2 ± 3.2	8.9 5.8	0.61 0.62
δ_2	14	1.77/0.20	67	693	1.14 ± 0.29	22.5	531 ± 210 214 ± 112	10.5 ± 1.9 11.4 ± 1.9	50.8 18.9	0.47 0.51

The α and β cells are remarkably homogeneous classes whereas the γ cells are likely to represent a morphologically heterogeneous population (Boycott & Wässle 1974) possibly corresponding to several different physiological classes (Cleland & Levick 1974a, b).

As explained previously we assume a passive spread of current in all cells, and that they all have the same membrane resistance, intracellular resistivity and membrane capacity. These assumptions will be discussed later.

3.1. Morphological and cable parameters

3.1.1. Dendritic–somatic surface, number of terminal branches, electrotonic length

Table 1 summarizes for the various ganglion cells some characteristic parameters. The ratio of dendritic surfaces to somatic surface D/S, the average dendritic field diameter d_t and the number of terminal branches n express some of the morphological differences between the cells that are obvious in figure 1. At the same eccentricity the ratio of dendritic to somatic surface seems a rather characteristic feature for each morphological class, though this observation should be verified on a larger sample of cells.

The number of terminal branches may be, on the other hand, quite characteristic for the β, γ and δ types, independently of eccentricity. In 16 α cells that we have examined we found that n = 97, 87, 61, 50, 55, 32, 53, 131, 126, 142 for ON cells and n = 45, 63, 37, 62, 29, 54 for OFF cells. In six β cells n = 48, 44, 45, 58 for ON cells and n = 44, 45 for OFF cells; in our four γ cells n = 16, 12, 16, 11; in our two δ cells n = 65, 67. This correlation has to be taken with care, however, since the number of terminal branches, especially thin ones, is the most likely parameter to be sensitive to the quality of staining.

In our representation of the dendritic tree the electrotonic length constant L is obtained simply by summating the electrotonic length l/λ associated with each dendritic segment from the soma to a given terminal branch. The values of L reported in table 1 are average values over all terminal branches of the neuron.

At 3 mm eccentricity the electrotonic length constant L is around 0.25 for the β and 0.65 for the α cell. Table 1 shows the values of L for all cells. Interestingly, the two β cells at 9 mm eccentricity have almost the same electrotonic length as the α cell at 3 mm eccentricity.

The simple interpretation of λ as an exponential decrement with distance (of d.c. signals) holds for branched trees only if they are equivalent to a cylinder. This last condition implies that the dendritic trunk parameter $\Sigma d_i^{\frac{3}{2}}$, where d_i is the diameter of each dendritic branch, must not change with the distance from the soma (Rall 1962). None of the ganglion cells that we examined is equivalent to a cylinder: their dendritic trunk parameter changes significantly with distance from the soma. In most cells $\Sigma d_i^{\frac{3}{2}}$ increases with increasing distance from the soma, reaches a maximum and then decreases. The increase of $\Sigma d_i^{\frac{3}{2}}$ with distance is due to daughter branches of a relatively large diameter: thus $\Sigma d_i^{\frac{3}{2}}$ is not preserved at branch points (in contrast to cat motoneurons, see Barrett & Crill 1974a). The parameter $\Sigma d_i^{\frac{3}{2}}$ decreases at greater distances mainly because of the termination of dendritic branches at different electrotonic lengths. Although the various ganglion cells show a different dependence of $\Sigma d_i^{\frac{3}{2}}$ on distance, the equivalent cylinder condition is clearly violated in all cases examined.

3.1.2. *Soma input impedance and transfer input impedances (steady state)*

Input and transfer resistances (d.c. impedances) are listed in table 1 as provided by our computer program. The α cell has by far the lowest soma d.c. input resistance consistently with its quite large dimensions. The β cell has a d.c. input resistance which decreases with eccentricity; its value, higher than for the α cell, is however, quite small compared with the size of the dendritic field. With much larger dendritic fields than have β cells, γ and δ cells have about the same input resistance.

Input impedances at the terminal tips can be very high and are quite variable within the same cell. The input resistance at the tip of the second centripetal branch (i.e. at the first branching from the terminal tip) is probably a better parameter. The α and β cells have similar values (at the same eccentricity) whereas γ and especially δ cells lie significantly higher (more than 100 MΩ and up to 200 MΩ for the dendritic tips at 9 mm eccentricity). The transfer resistance from the dendrites to the soma is higher for β than for α cells, roughly reflecting the soma input resistance values.

The voltage attenuation from the tips and from the tips of the second centripetal branch to the soma (see §2) summarizes most of these electrical properties. At 3 mm eccentricity the α cell shows the highest attenuation, whereas voltage in the β cells experiences only a slight attenuation (from the second centripetal branch the attenuation is 2 compared with 10 for

the α cell). The γ and δ cells lie in between, with the more branched δ cell showing a higher attenuation than the γ cell. Attenuation increases with cell dimensions and therefore with eccentricity.

3.1.3. *Subunits*

Transfer resistance values for many different pairs of locations on the dendritic tree can be visualized in terms of the subunit maps shown in figures 2–6 for some of the ganglion cells

position of i, j	$K_{i,j}/\mathrm{M\Omega}$	$K^{\mathrm{eff}}_{i,j}/\mathrm{M\Omega}$
1, 1	59.2 (75.7)	43.6
1, s	3.1 (12.7)	0.9
2, 2	42.2 (57.9)	28.7
2, s	3.2 (12.8)	0.9
2, 5	15.9 (29.4)	8.6
5, 5	18.1 (30.6)	10.4
2, 9	4.7 (15.2)	1.7
9, 9	37.4 (49.8)	29.3
s, s	5.7 (15.7)	2.2
2, 7	2.4 (11.6)	0.7
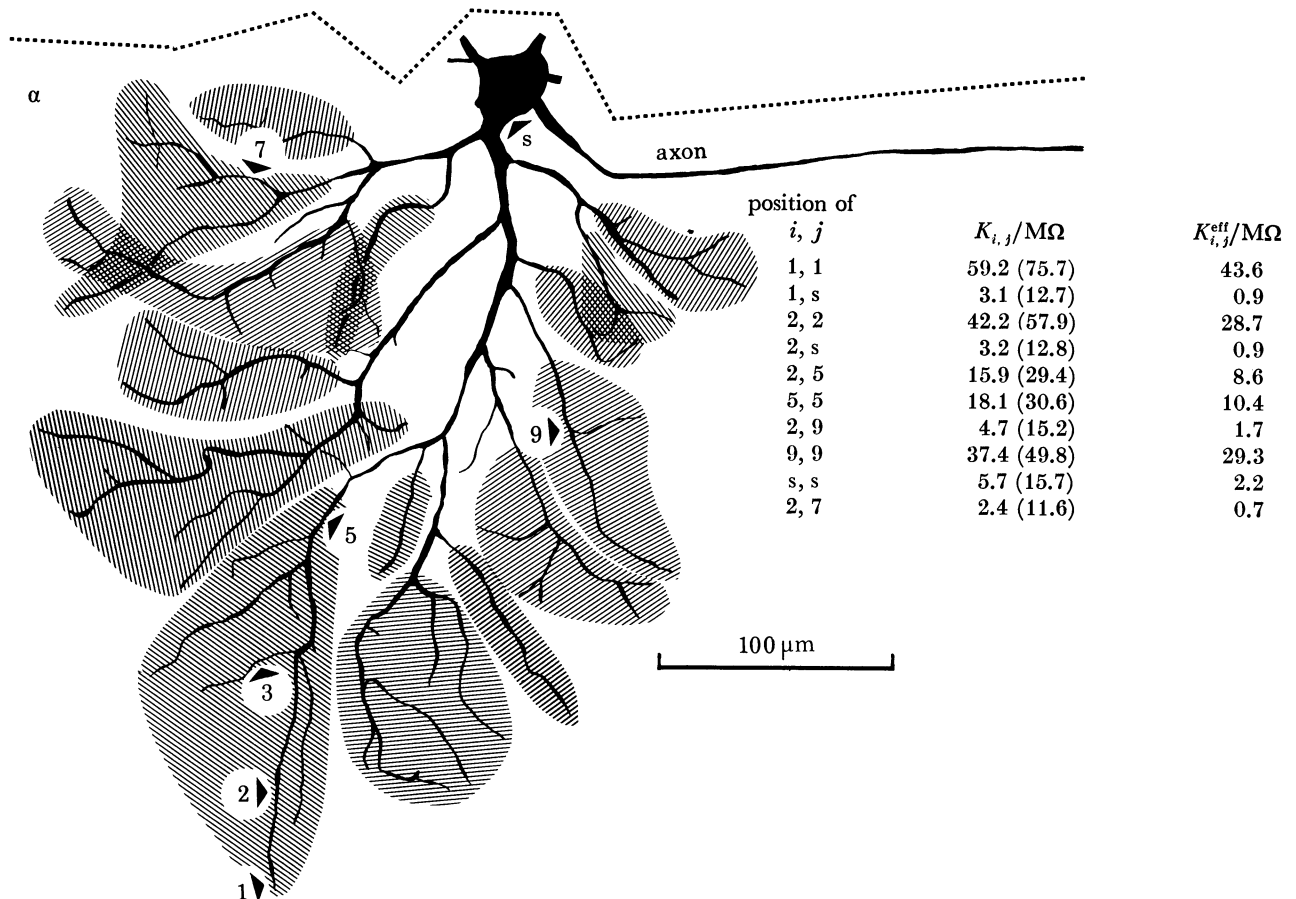
Figure 2. A part of the α cell of figure 1, at higher magnification. A set of subunits is shown here for $R_{\mathrm{m}} = 2500\ \Omega$ cm² and for $c = 4$ (see text). It illustrates regions that can be considered to be equipotential. Intersecting subunits refer to dendrites which overlap with a depth difference of no more than 3 μm. Representative values for input and transfer resistances at various locations are shown. Values for K^{eff} refer to transient inputs with $t_{\mathrm{peak}} = 1$ ms. Values in parentheses refer to $R_{\mathrm{m}} = 8000\ \Omega$ cm².

studied. The picture that emerges can be readily summarized. The α cell, despite the small electrotonic dimensions ($L \approx 0.65$) is clearly not equipotential, showing distinct subunits (see figure 2). Its total number of subunits is 32 with our criterion ($c = 4$). Estimates of average transfer and input resistances of subunits are quite useful for characterizing the functional properties of subunits, although the computational procedure is somewhat arbitrary. To obtain $\langle K_{ii} \rangle$, the average input resistances and transfer resistances at various points within each subunit were weighted according to the length of the associated branch. The values obtained were then averaged among all subunits.

In a similar way we computed $\langle K_{ij} \rangle$ as the weighted transfer resistance between two different subunits. As illustrated for a few cases in the corresponding figure 2, transfer and input (d.c.) resistances within a subunit are sizable (the average $\langle K_{ii} \rangle$ for all subunits is estimated to be around 55 ± 10 MΩ), whereas transfer resistances between different subunits and between each subunit and the soma are very low (weighted average of K_{ij} is about 2.6 MΩ, with a range from 8 MΩ for near subunits to 1 MΩ for far subunits, whereas $\langle K_{is} \rangle$ is 4.0 ± 1.0 MΩ). The branching of α cells from large trunks to thin dendrites, together with the relatively long

position of i, j	$K_{i,j}/$MΩ	$K_{i,j}^{\text{eff}}/$MΩ
1, 1	143.0 (204.8)	116.4
1, 5	29.0 (89.2)	9.9
1, 2	80.6 (142.5)	55.4
2, 2	149.6 (212.5)	54.8
1, 3	80.1 (141.6)	54.8
3, 3	80.4 (141.8)	55.1
4, 4	66.6 (127.5)	41.7
4, s	29.7 (99.9)	10.2
s, s	31.0 (91.2)	10.7
4, 3	27.9 (88.1)	9.5
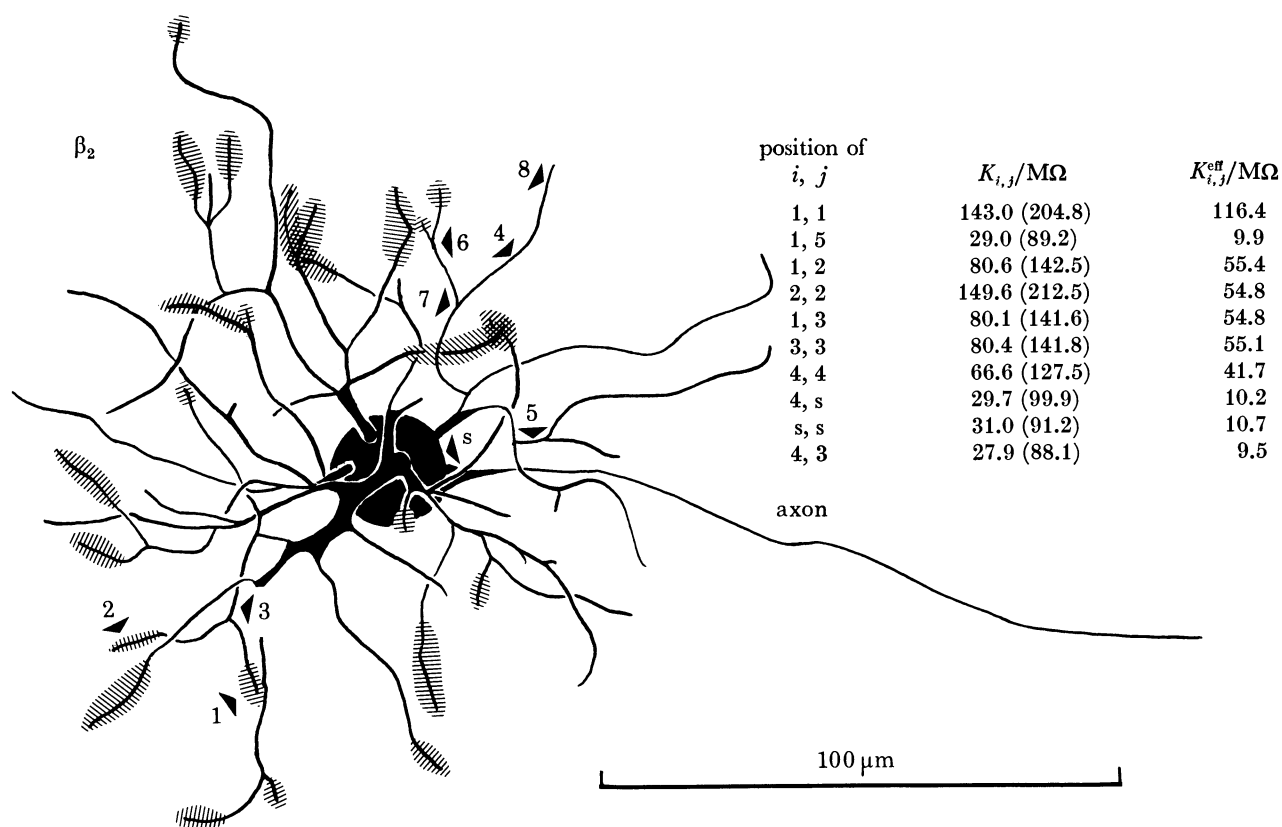
FIGURE 3. As figure 2, for the β_2 cell of figure 1. Unlike the α cell, this neuron is rather equipotential with small subunits. Notice that the whole β cell has roughly the size of an α subunit.

branches, is the main reason for the electrical decoupling of the subunits. In comparison, γ cells of about the same overall spread but with a different pattern of branching have a quite different subunit map.

At the same eccentricity β cells do not have any subunits of a significant size. Figure 3 shows the largest of the two β cells of figure 1. Input resistances are relatively constant over the whole cell (our estimate of the average $\langle K_{ii} \rangle$ is around 70 MΩ for β_2). The other β cell at the same eccentricity (β_1) has even fewer and smaller subunits and somewhat lower transfer resistances ($\langle K_{ii} \rangle \approx 55$ MΩ). Thus β cells at this or smaller eccentricities tend to be equipotential with input resistances that are quite homogeneous. This is due primarily to the small electrotonic dimensions of the β cells and also to their short, relatively stout distal branches. The addition of a thin and long (50 µm) dendrite to the β cell of figure 3 would create a sizable subunit with a tip input impedance around 400 MΩ. Interestingly, with our criterion the size of the

whole β cell is roughly comparable to the size of an α subunit. Notice that if a β cell is systematically expanded, by making lengths and diameters larger while maintaining the same branching geometry, large subunits appear.

One of the two γ cells (γ_2) of figure 1 is shown in figure 4 with its subunits and typical transfer resistance values. Within the subunits, d.c. transfer and input resistances are well above 100 MΩ (the average $\langle K_{ii} \rangle$ within subunits is around 213 $\pm$ 100 MΩ) whereas the rest of the cell is equipotential with typical transfer resistances around 30–40 MΩ (the average $\langle K_{is} \rangle$ is 28 $\pm$ 6 MΩ,

position of i, j	$K_{i,j}/$MΩ	$K_{i,j}^{\text{eff}}/$MΩ
1, 1	217.2 (314.4)	142.9
1, s	23.1 (91.7)	7.1
1, 2	103.2 (192.0)	57.3
2, 2	112.8 (197.5)	64.2
2, s	25.2 (94.3)	7.8
1, 7	26.5 (97.3)	9.0
7, 7	184.0 (269.4)	131.8
s, s	37.4 (108.2)	13.8
2, 8	17.2 (83.0)	
1, 4	156.7 (251.4)	
2, 5	95.5 (178.4)	
5, 5	99.1 (180.6)	
5, s	26.1 (95.5)	

100 μm
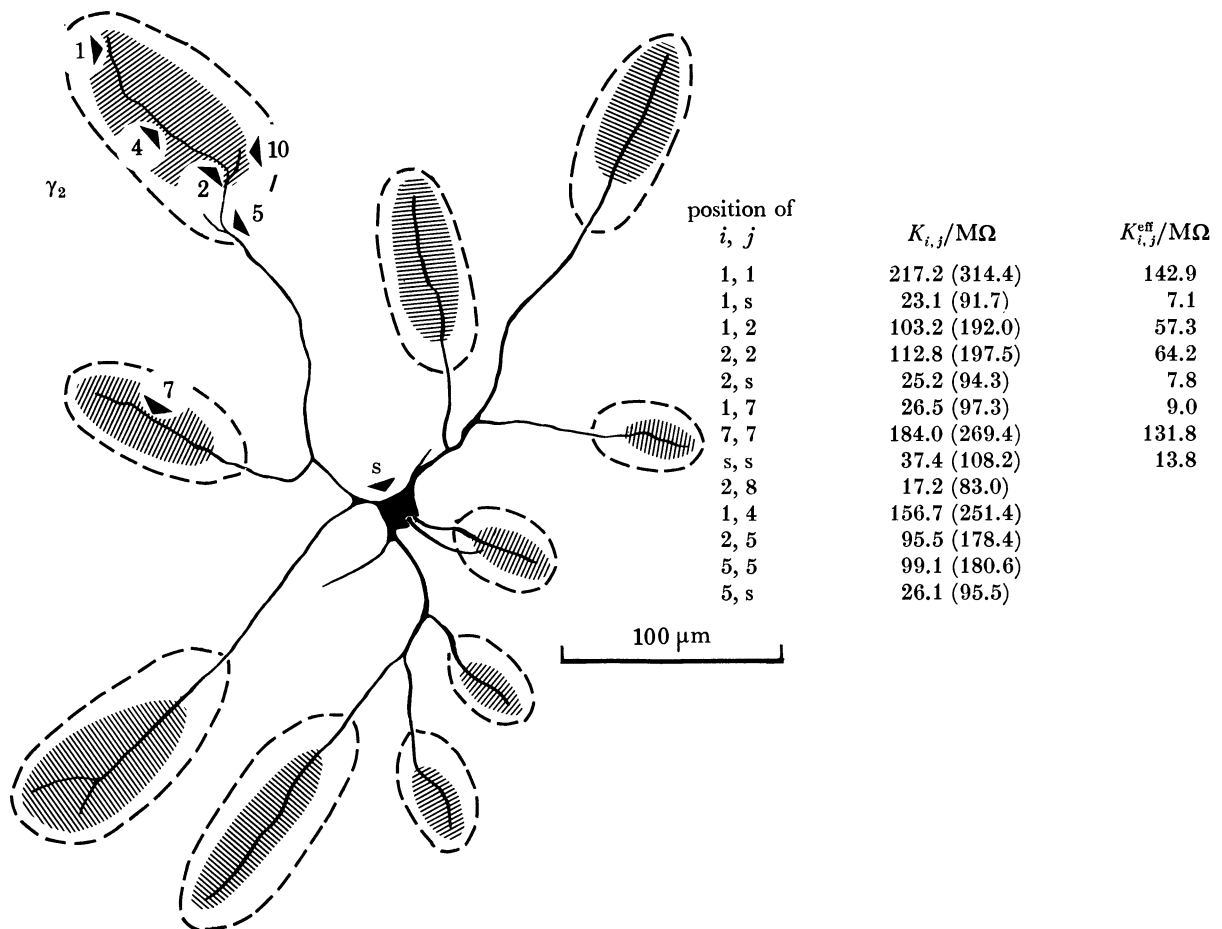
FIGURE 4. As figure 2, for the γ_2 cell of figure 1. Dotted lines indicate the subunits obtained for $c = 3$ (see text).

while the average $\langle K_{ij} \rangle$ is 21 $\pm$ 7 MΩ). The γ subunits are distinguished from α and β subunits by their higher input and transfer resistance values.

A δ cell at the same etcentricity (see figure 1) is shown in figure 5. Despite an overall dendritic field-area that is less than half the area of the α cell, it has 23 subunits. The type of dendritic tree, with daughter branches of almost the same small diameter as the mother branches, is the main reason for this. Notice that the electrotonic length of this cell is very similar to the α cell electrotonic length despite the smaller dimensions of the dendritic field, since the diameters of the branches are smaller. Within each subunit electrical coupling is quite high (the estimate

for the weighted average $\langle K_{ii} \rangle$ within subunits is 114 MΩ). Transfer resistances from subunits to the soma are low ($\langle K_{is} \rangle \approx 16$ MΩ); from one subunit to another $\langle K_{ij} \rangle \approx 14$ MΩ with a range from 8 MΩ for far subunits to 42 MΩ for neighbouring ones.

3.1.4. Subunits and eccentricity

Figure 6 shows an ON β cell located at an eccentricity of 9 mm. As is true also for α cells, the dendritic field of β cells become larger with increasing eccentricity, and they become

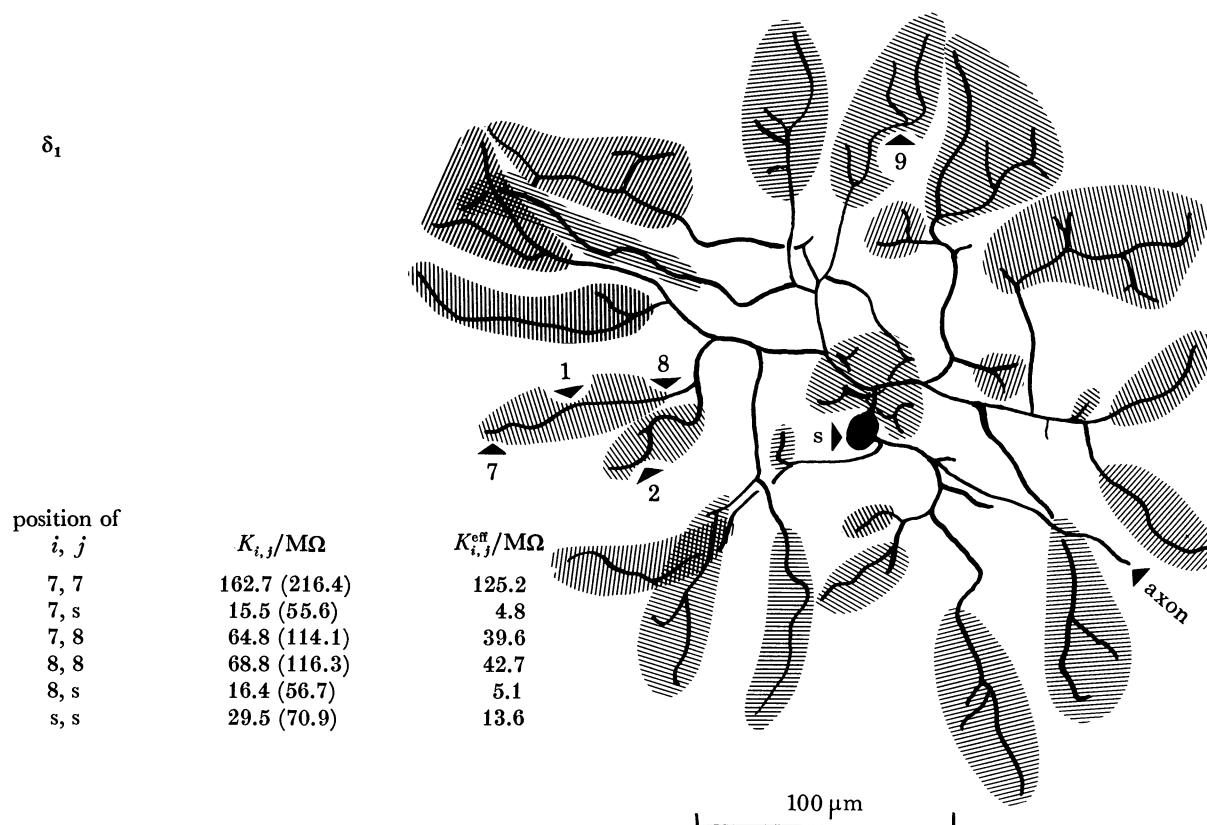| position of i, j	$K_{i,j}$/MΩ	$K_{i,j}^{\text{eff}}$/MΩ
7, 7	162.7 (216.4)	125.2
7, s	15.5 (55.6)	4.8
7, 8	64.8 (114.1)	39.6
8, 8	68.8 (116.3)	42.7
8, s	16.4 (56.7)	5.1
s, s	29.5 (70.9)	13.6

FIGURE 5. As figure 2, for the δ_1 cell of figure 1.

correspondingly more inhomogeneous electrically, with subunits appearing and increasing in number. Boycott & Wässle (1974; personal communication) point out that eccentric β cells are morphologically quite similar to α cells nearer to the area centralis. Our data suggest that this similarity extends to their respective passive electrical properties (cf. Lennie 1980).

3.1.5. ON–OFF β cells

Wässle et al. (1981 a, b) and Peichl & Wässle (1981) have recently classified their α and β cells in terms of ON–OFF properties (see also Famiglietti et al. 1977; Nelson et al. 1978). We have analysed the morphology of a pair of β cells at the same eccentricity, one ON, the other OFF (Wässle et al. 1981 a) to look for differences in their cable properties. Again, a similar morphology of the dendritic tree is reflected in quite similar electrical properties.

3.1.6. *Transient inputs*

The electrical properties discussed so far all refer to steady state d.c. inputs. In practice they hold for inputs with a time course that is slow relative to the time constants characteristic for the various cells. For transient inputs with a time to peak longer than 30 ms all cells show electrical properties, such as voltage attenuation, within 5 % of their d.c. values (the input time course used was of the type

$$t^n e^{-t/t_{\text{peak}}}, \quad n = 1\text{--}4).$$

Since the light evoked postsynaptic potentials in ganglion cells have a time to peak usually longer than 20–40 ms, our steady state data can probably be used for all light evoked responses.
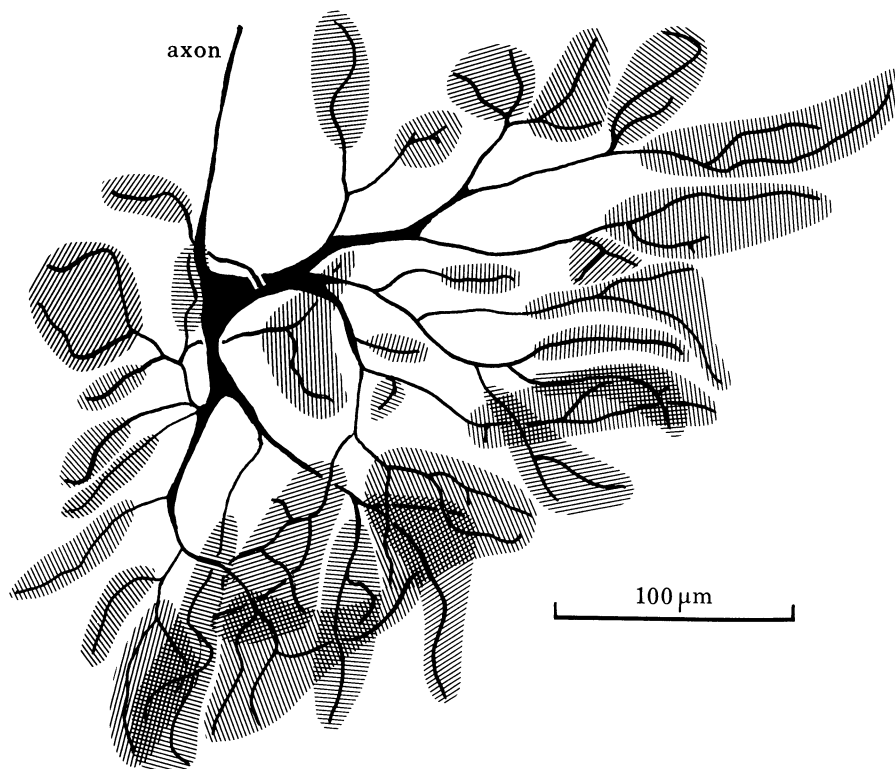

FIGURE 6. As figure 2, for the β_4 cell at 9 mm eccentricity (see table 1 and text).

The d.c. approximation is no longer valid for very brief transients. As explained in §2.1, we have computed the 'effective' resistances K^{eff} for short transient inputs, similar to unitary postsynaptic potentials, with a time course

$$t e^{-t/t_{\text{peak}}}, \quad t_{\text{peak}} = 1 \text{ ms}.$$

The values of K^{eff} can be used with the d.c. formulae of §2.3 to obtain very good approximations to nonlinear effects for transient inputs, such as nonlinear saturation. The values of K^{eff} shown in figures 2–5 for specific locations illustrate the effective resistance of the various cells for these fast transients. Together with the d.c. values they give an upper and a lower bound for the attenuation factors involved over a wide range of input time courses. Transfer and input resistances are of course lower for the transient than for the d.c. case. The difference between very fast transients and d.c. inputs is larger for increasing distance between locations

of the input current and of the output voltage, as an effect of electrotonic distance and branching (Rinzel & Rall 1974). Transfer input resistances to the soma and soma input resistances are more affected (relative to their d.c. values) than input resistances at the tips of the dendrites. Voltage attenuation from distal to proximal locations is therefore substantially greater for transient case than for d.c. inputs (figures 2–5).

As a consequence the electrical properties of all ganglion cells are spatially even more inhomogeneous for transient than for d.c. inputs. The difference between transient inputs and d.c. inputs is of the same order for all types of cells. In all cells voltage attenuation (A_V) for distal inputs increases from d.c. to transients by about a factor 2. The subunit maps of figures 2–6 change of course for a transient input, subunits becoming larger. The qualitative picture, especially concerning the relative differences among the various types remains, however, basically similar $(c = 4$ for transients yields similar subunit size for same cells as $c = 2.8$ for d.c.). Finally, it is noteworthy that the voltage attenuation has its minimum d.c. value for inputs with a time course comparable to light evoked inputs, whereas it increases quickly for shorter transients. Thus dendrites of ganglion cells behave as low pass filters with a cutoff frequency apparently well suited to increasing the ratio between light induced signals and the synaptic noise.

3.1.7. Charge transfer and relative effectiveness of dendritic synapses

The fraction of charge that is transferred from synapses to the soma for transient inputs is an important parameter to characterize the effectiveness of synapses. In the cat motoneurons the firing rate at the soma depends rather directly on the depolarizing current reaching the soma (see Redman 1976). In ganglion cells of the turtle retina the frequency of firing increases linearly with injected current strength above a certain rheobase value (Baylor & Fettiplace 1979).

The fraction Q of charge delivered to the soma is independent of the time course of current injection (Rinzel & Rall 1974; Barrett 1975). We have shown that $Q = K_{is}/K_{ss}$. Therefore the fraction of charge delivered in the soma by arbitrary transients can be computed in terms of steady state properties of the neuron (the d.c. resistances K_{is} and K_{ss}). The factor Q, the synaptic effectiveness, is very high for all ganglion cells (also for $R_m = 2500 \ \Omega \ cm^2$). The most distal synapses are 47 % as effective as somatic synapses for the peripheral δ cell and much more than that for the other cells. Synaptic effectiveness is maximal in β cells (above 75 %) and minmal in δ cells (around 50 %); it is surprisingly high in the α cell (above 70 %). Figure 7 shows that the charge factor does not vary much with distance from the soma when the membrane resistance is higher than 2500 $\Omega \ cm^2$ (in the illustrative case of one specific branch of the γ cell of figure 4). These values suggest that dendritic synapses have a functional role of primary importance for all ganglion cells, even for transient distal inputs. Interestingly, Iansek & Redman (1973) found that, for unitary Ia excitatory postsynaptic potentials in cat motoneurons, delivered somatic charge is almost independent of synaptic location. Finally, it is interesting that a voltage change in the soma depolarizes a distal dendritic location proportionally to the associated factor Q. Thus the effect of the antidromic passive spread of somatic action potentials is maximal for α and β cells (for which firing activity is also higher).

3.2. Nonlinear effects of conductance inputs: significance of dendritic architecture

Within regions of the dendritic tree characterized by high input and transfer resistances specific nonlinear effects for conductance inputs may be considerable. Using the formulae

derived in an earlier section we have estimated the degree of nonlinear addition (i.e. saturation) and of nonlinear interaction to be expected for the cells of figures 2–6. We will discuss later the possible computational role of these properties.

3.2.1. *Nonlinear addition*

As shown in §2.3.1 a conductance change g at location i induces a voltage in the soma given by

$$V_{\mathrm{s}} = gK_{is}E/(1+gK_{ii}), \tag{3.1}$$

where E is the driving potential at location i. The data of table 1 and the average values of $\langle K_{ii}\rangle$ and $\langle K_{is}\rangle$ allow us to compare the different cells. For very small values of g, in equation
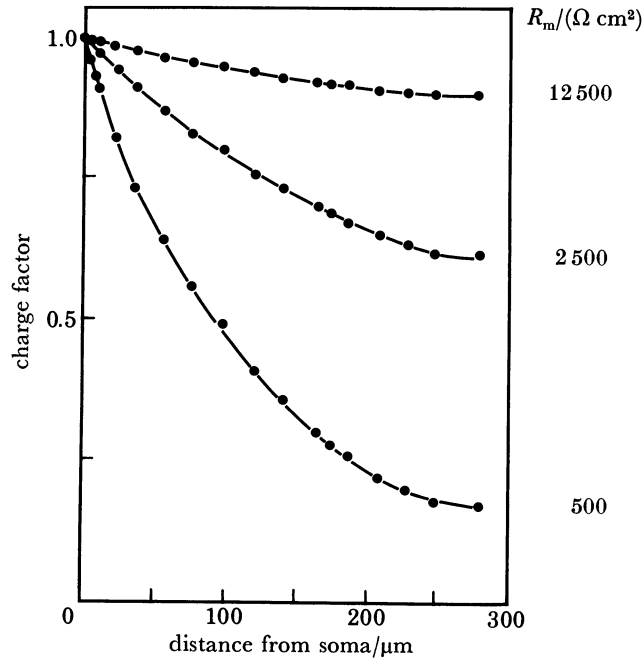

FIGURE 7. Charge factor $Q = K_{is}/K_{ss}$ for different values of the membrane resistance as a function of the distance of the input current location from the soma along the branch indicated by (1–4–2–5–s) on the γ cell of figure 4 (γ_2).

(3.1) $V_{\mathrm{s}} \approx gK_{is}E$. Under these conditions equal synapses (i.e. synapses having the same g and E) on distal dendrites of β and γ cells are almost equally effective, being 10 times more efficient than in α cells and 1.5–2 times more efficient than in δ cells.

For very large synaptic inputs $(g \to \infty)$, the voltage potential in the soma can be approximated as

$$V_{\mathrm{s}} = (K_{is}/K_{ii})E$$

and K_{is}/K_{ii} can be taken as a measure of maximal synaptic efficiency. The α cell is again the least efficient cell $(K_{is}/K_{ii}$ is 0.039, 0.095 and 0.056 for a synapse located at the terminal tip, at the tip of second centripetal branch and distributed on one subunit, respectively). The β cells become the most effective (the corresponding values of K_{is}/K_{ii} are 0.28, 0.53, ≈ 1 for β_1. The difference between γ and δ cells is less pronounced $(K_{is}/K_{ii}$ for γ_2 is 0.11, 0.17 and 0.14).

If the conductance g is distributed among N subunits, the voltage potential at the soma becomes

$$V_{\mathrm{s}} = g\langle K_{is}\rangle E/(1+g\langle K_{ii}^{av}\rangle)$$

with

$$\langle K_{ii}^{av}\rangle = [\langle K_{ii}\rangle + (N-1)\langle K_{ij}\rangle]/N.$$

In this case the synaptic efficiency for small conductance changes remains the same but the maximal synaptic efficiency increases now to $\langle K_{is}\rangle/\langle K_{ii}\rangle$. The factor $G = \langle K_{ii}\rangle/\langle K_{ii}^{av}\rangle$ gives a measure of the reduction in saturation, which can be achieved by distributing the same conductance change over all subunits. Using the electrical parameters estimated in §3.1.3 for the subunits of the various cells we can now compute the associated values of G. In the α cells $G = 13.1$, giving an overall maximal synaptic efficiency of 0.73, as a consequence of reduced synaptic saturation within each subunit. The number and area of subunits in β cells is too small to justify a calculation of the same type. The value of G for the γ cell is 5.3 and for the δ cell 6.2.

All these estimates were derived under our standard assumption of $R_{\mathrm{m}} = 2500\ \Omega\ \mathrm{cm}^2$. For membrane resistance values around $8000\ \Omega\ \mathrm{cm}^2$ or larger, subunits disappear almost completely in all cells (for $c = 4$). In this case saturation cannot be very substantially reduced by spreading the same input conductance among subunits.

In addition to the voltage depolarization induced in the soma considered so far, it is interesting to estimate the amount of current that flows from location i to the soma. The current I_i at location i is

$$I_i = gE/(1+gK_{ii})$$

and the current reaching the soma is then

$$I_{\mathrm{s}} = gK_{is}E/K_{ss}(1+gK_{ii}),$$

i.e.

$$I_{\mathrm{s}} = QgE/(1+gK_{ii}).$$

Thus the maximal current that can reach the soma from a synapse located in i is

$$K_{is}E/K_{ss}K_{ii}$$

(for $g \to \infty$). Using the average estimated values of the subunits for K_{is} and K_{ii}, the maximal current is for the α cell $0.0084 \times 10^{-6}\ \mathrm{S}\ E$, for the β $0.0135 \times 10^{-6}\ \mathrm{S}\ E$, for the γ cell $0.0035 \times 10^{-6}\ \mathrm{S}\ E$ and for the δ cell $0.0047 \times 10^{-6}\ \mathrm{S}\ E$. When the same conductance change g is distributed over all the available subunits and $\langle K_{ii}\rangle$ is substituted with $\langle K_{ii}^{av}\rangle$ the α cell becomes the most powerful of the cells for injecting current in the soma.

3.2.2. Nonlinear interactions

A distal excitatory input can be effectively shunted by an inhibitory input on the path to the soma, when the inhibitory battery is assumed to be around the resting potential ($E_i \approx 0$). In all ganglion cells the relatively high transfer impedances in the distal branches can underly strong nonlinear interactions offering the possibility of synthesizing local circuits performing a variety of operations. In particular, inhibitory inputs in the proximal part of a subunit can specifically shunt more distal excitatory inputs on the same subunit. This module would be capable of performing a kind of multiplication (see Poggio & Torre 1978) between the two types of inputs, in effective isolation from other subunits. Such a module may underlie, for instance, the property of directional selectivity to motion in some ganglion cells. We have

TABLE 2. F VALUES FOR D.C. EXCITATION (AT LOCATION 2)
AND SHUNTING INHIBITION IN THE α CELL OF FIGURE 2

(R_m = 2500 Ω cm². The depolarization at the soma due to excitation alone (for E_e = 80 mV) is 5.8 mV for g_e = 10^{-6} S, 4.8 mV for g_e = 10^{-7} S, 1.8 mV for g_e = 10^{-8} S and 0.2 mV for g_e = 10^{-9} S.)

$g_e/(10^{-6}$ S) ...	0.001	0.01	0.1	1.0	→ ∞	0.001
$g_i/(10^{-6}$ S) ...	0.1	0.1	0.1	0.1	0.1	0.001
inhibition						
at 1	2.39	2.02	1.28	1.03	1.00	1.04
2	5.05	3.97	1.81	1.09	1.00	1.04
3	1.69	1.58	1.37	1.30	1.29	1.02
5	2.79	2.64	2.33	2.23	2.21	1.02
s	1.56	1.56	1.55	1.54	1.54	1.01
7	1.07	1.07	1.07	1.07	1.07	1.00
$g_e/(10^{-6}$ S) ...	0.1	0.1	0.1	0.1	0.1	0.001
$g_i/(10^{-6}$ S) ...	0.001	0.01	0.1	1.0	→ ∞	0.01
inhibition						
at 1	1.01	1.06	1.28	1.41	1.43	1.33
2	1.01	1.08	1.81	9.08	∞	1.40
3	1.01	1.11	1.37	1.50	1.52	1.20
5	1.01	1.13	2.33	14.27	∞	1.18
s	1.00	1.05	1.55	6.48	∞	1.06
7	1.00	1.02	1.07	1.09	1.09	1.02

TABLE 3. F VALUES FOR D.C. EXCITATION (AT LOCATION 4)
AND SHUNTING INHIBITION IN THE β₂ CELL OF FIGURE 3

(R_m = 2400 Ω cm². The depolarization at the soma due to excitation alone (for E_e = 80 mV) is 35.2 mV for g_e = 10^{-6} S, 31.0 mV for g_e = 10^{-7} S, 14.3 mV for g_e = 10^{-8} S and 2.2 mV for g_e = 10^{-9} S.)

$g_e/(10^{-6}$ S) ...	0.001	0.01	0.1	1.0	→ ∞	0.001
$g_i/(10^{-6}$ S) ...	0.1	0.1	0.1	0.1	0.1	0.001
inhibition						
at 8	3.25	2.44	1.31	1.03	1.00	1.06
4	7.24	4.99	1.87	1.09	1.00	1.06
6	1.68	1.50	1.26	1.20	1.19	1.04
7	5.67	4.48	2.82	2.41	2.35	1.05
s	4.02	3.57	2.95	2.78	2.78	1.03
5	2.52	2.27	1.93	1.84	1.84	1.03
$g_e/(10^{-6}$ S) ...	0.1	0.1	0.1	0.1	0.1	0.001
$g_i/(10^{-6}$ S) ...	0.001	0.01	0.1	1.0	→ ∞	0.01
inhibition						
at 8	1.01	1.07	1.31	1.46	1.48	1.53
4	1.00	1.08	1.87	9.69	∞	1.62
6	1.02	1.11	1.26	1.30	1.30	1.29
7	1.02	1.18	2.82	14.16	∞	1.47
s	1.02	1.19	2.95	20.51	∞	1.30
5	1.02	1.17	1.93	2.67	2.84	1.28

computed the steady state degree of nonlinear interaction F for some locations of inhibition and excitation in the various cells, assuming values for the d.c. conductance inputs of g_e = 10^{-7} S with g_i varying from 10^{-9} S to 10^{-5} S and of g_i = 10^{-7} S with g_e varying from 10^{-9} S to 10^{-5} S (see tables 2–5). Recall that in cat motoneurons the peak amplitude of a quantal postsynaptic conductance change is estimated to be between about 10^{-8} and 10^{-7} S (Barrett 1975) whereas an

TABLE 4. F VALUES FOR D.C. EXCITATION (AT LOCATION 4)

AND SHUNTING INHIBITION IN THE γ CELL OF FIGURE 4

(For a comparison R_m values of (a) 2500 and (b) 8000 Ω cm² are shown here. Similar effects of increasing R_m can be seen in the other cells. For R_m = 2500 Ω cm² the depolarization at the soma due to excitation alone (for E_e = 80 mV) is 11.7 mV for g_e = 10^{-6} S, 11.1 mV for g_e = 10^{-7} S, 7.2 mV for g_e = 10^{-8} S and 1.6 mV for g_e = 10^{-9} S. For R_m = 8000 Ω cm² the depolarization at the soma due to excitation alone (for E_e = 80 mV) is 29.0 mV for g_e = 10^{-6} S, 28.1 mV for g_e = 10^{-7} S, 20.9 mV for g_e = 10^{-8} S and 5.9 mV for g_e = 10^{-9} S.)

(a) R_m = 2500 Ω cm²

$g_e/(10^{-6}$ S) ...	0.001	0.01	0.1	1.0	$\to \infty$	0.001
$g_i/(10^{-6}$ S) ...	0.1	0.1	0.1	0.1	0.1	0.001
inhibition						
at 1	2.78	1.79	1.12	1.01	1.00	1.12
4	14.82	7.16	1.94	1.10	1.00	1.14
2	11.32	7.99	5.73	5.36	5.32	1.10
10	3.47	2.68	2.14	2.05	2.04	1.10
7	1.18	1.17	1.16	1.16	1.16	1.03
s	4.69	4.52	4.41	4.39	4.39	1.04

$g_e/(10^{-6}$ S) ...	0.1	0.1	0.1	0.1	0.1	0.001
$g_i/(10^{-6}$ S) ...	0.001	0.01	0.1	1.0	$\to \infty$	0.01
inhibition						
at 1	1.01	1.05	1.12	1.14	1.14	1.80
4	1.01	1.09	1.94	10.41	∞	2.38
2	1.05	1.47	5.73	48.27	∞	2.03
10	1.05	1.36	2.14	2.46	2.50	1.78
7	1.02	1.11	1.16	1.17	1.17	1.12
s	1.03	1.34	4.41	35.15	∞	1.37

(b) R_m = 8000 Ω cm²

$g_e/(10^{-6}$ S) ...	0.001	0.01	0.1	1.0	$\to \infty$	0.001
$g_i/(10^{-6}$ S) ...	0.1	0.1	0.1	0.1	0.1	0.001
inhibition						
at 1	3.66	1.94	1.13	1.01	1.00	1.19
4	21.20	8.16	1.96	1.10	1.00	1.20
2	17.76	10.16	6.54	6.04	5.98	1.17
10	5.03	3.21	2.34	2.22	2.21	1.16
7	1.56	1.44	1.39	1.38	1.35	1.08
s	11.13	9.40	8.57	8.46	8.45	1.10

$g_e/(10^{-6}$ S) ...	0.1	0.1	0.1	0.1	0.1	0.001
$g_i/(10^{-6}$ S) ...	0.001	0.01	0.1	1.0	$\to \infty$	0.01
inhibition						
at 1	1.00	1.06	1.13	1.14	1.15	2.21
4	1.00	1.09	1.96	10.62	∞	3.02
2	1.05	1.55	6.54	56.40	∞	2.68
10	1.05	1.42	2.34	2.72	2.77	2.27
7	1.05	1.26	1.39	1.41	1.37	1.34
s	1.07	1.75	8.57	76.74	∞	2.01

acetylcholine quantum in the skeletal neuro-muscular synapse induces a peak conductance change of about 2.5×10^{-8} S (Hartzell et al. 1976; Stevens 1976).

With the values of K typical for our cells, conductance changes of the order of 10^{-9} S are clearly in the linear range, whereas conductance values around 10^{-6} S approach the asymptotic case of $g \to \infty$. Therefore, the conductance values considered in tables 2–5 represent the whole relevant range of inputs.

All cell types show the general properties of shunting inhibition listed in §2.3.2. In particular, inspection of the tables 2–5 shows that:

(i) For excitatory conductance changes of around 10^{-9} S the optimal location of the inhibition is on the same site as the excitation (R_m = 2500 and 8000 Ω cm^2). For weak excitation the interaction is very local and specific. F mainly depends on the distance between the two synapses.

TABLE 5. F VALUES FOR D.C. EXCITATION (AT LOCATION 1)
AND SHUNTING INHIBITION IN THE δ CELL OF FIGURE 5

(R_m = 2500 Ω cm^2. The depolarization at the soma due to excitation alone (for E_e = 80 mV) is 11.6 mV for g_e = 10^{-6} S, 10.7 mV for g_e = 10^{-7} S, 6.1 mV for g_e = 10^{-8} and 1.1 mV for g_e = 10^{-9} S.)

$g_e/(10^{-6}\ S)$ ...	0.001	0.01	0.1	1.0	$\to \infty$	0.001
$g_i/(10^{-6}\ S)$ ...	0.1	0.1	0.1	0.1	0.1	0.001
inhibition						
at 7	2.37	1.72	1.12	1.01	1.00	1.09
1	10.75	6.19	1.91	1.09	1.00	1.10
8	7.48	5.78	4.17	3.87	3.83	1.06
2	1.58	1.46	1.35	1.32	1.32	1.05
9	1.16	1.15	1.14	1.14	1.14	1.01
s	3.92	3.82	3.73	3.71	3.71	1.03
$g_e/(10^{-6}\ S)$ ...	0.1	0.1	0.1	0.1	0.1	0.001
$g_i/(10^{-6}\ S)$ ...	0.001	0.01	0.1	1.0	$\to \infty$	0.01
inhibition						
at 7	1.00	1.05	1.12	1.15	1.15	1.59
1	1.00	1.09	1.91	10.15	∞	1.98
8	1.03	1.31	4.17	32.90	∞	1.65
2	1.02	1.17	1.35	1.34	1.39	1.28
9	1.01	1.07	1.14	1.15	1.16	1.08
s	1.02	1.27	3.73	28.34	∞	1.29

(ii) When the excitatory conductance change increases up to 10^{-6} S the optimal location of inhibition moves towards the soma, but only in the β cell is inhibition maximal at the soma. This is probably due to the small size of the β cell (at the same eccentricity of 3 mm). When R_m grows to 8000 Ω cm^2 somatic inhibition becomes optimally effective except for the α cell, where even for $g_e \to \infty$ non-somatic inhibition on the direct path is more effective.

(iii) For very large excitatory inputs ($g_e \to \infty$) all locations of inhibition behind the excitatory input are essentially ineffective. When $g_e > 10^{-7}$ S all inhibitory synapses located behind the excitatory synapse are less effective than all other locations. For instance, the resulting F value is lower when the inhibitory synapse is 10 μm more distal than the excitatory synapse on the same path than when it is located at the tip of any other dendrite. This effect, which is mainly due to the branching geometry, increases for R_m = 8000 Ω cm^2.

(iv) Inhibition on the direct path is significantly more effective than at any other location. The specificity of 'on path location' is maximal for γ and δ cells. In α and β cells the effect becomes clear for larger inhibitory inputs ($g_i \approx 10^{-6}$ S). This property holds true also for much higher values of R_m (for instance R_m = 8000 Ω cm^2, see table 4b). Y-branches present a special problem. Inhibition very near the branch point can affect excitation on the other branch, even though it does not lie on the direct path. Its effectiveness, however, decreases very

rapidly with increasing distances from the branch point. In δ cells distances above 20 μm reduce drastically the effectiveness of inhibition. If the inhibitory (shunting) synapse is on a spine its effectiveness is considerably reduced compared to a location directly on the dendrite. In a dendrite of a γ cell, for instance, F can decrease to about 50 %, when the inhibitory input is on a dendritic spine, 1 μm in length, 0.2 μm in neck diameter.

(v) Inhibition can be extremely effective in shunting larger excitatory inputs, provided that its absolute size is around 10^{-7} S or greater. An inhibitory synapse on the direct path to the soma can shunt an excitatory input ten times as large with a factor F between 2 and 6. This effect is quite strong in γ ($F \approx 5.5$) and δ cells ($F \approx 3.8$), while it is relatively weak for α ($F \approx 2.0$) and β ($F \approx 2.5$) cells. Effectiveness of inhibition is maintained and actually enhanced by larger R_m values. Interestingly, cable properties are essential for the high effectiveness of inhibition against large excitatory inputs: in a lumped membrane circuit (or in a cable structure with coincident location of excitation and inhibition) the asymptotic value of F for very large g_e and g_i can be shown to be $s + 1$, where s is the ratio between inhibition and excitation ($s = g_i/g_e$). Thus, for $g_e = g_i$, $F = 2$ and for $g_e = 10 g_i$, $F = 1.1$ in a lumped circuit, whereas much higher values can be obtained in a dendritic tree (see tables). The notion of the subunit introduced in §2.2 had an important role in our discussion of saturation effects for synaptic inputs of one type. Somewhat surprisingly, the subunit idea is only of secondary importance for analysing synaptic interactions between excitation and shunting inhibition. Here the critical condition for strong interactions is that inhibition lies on the direct path to the soma. As a consequence, an inhibitory input can be considered very 'close' to excitation, from the point of view of nonlinear interactions, whever it is located on the direct path to the soma. Different subunits are usually well decoupled from this point of view also, but within any given subunits, however electrically homogeneous, there is a finer structure when inhibition is considered, arising from the *direct path* condition. The data of tables 2–5 reveal that this 'fine structure' is especially marked in γ and δ cells when compared with α and β cells. In δ cells compared with γ cells, inhibition can more specifically veto distal excitatory inputs, because of their higher branching frequency.

Interestingly the passive spread of depolarization induced by somatic firing may decrease the nonlinearity of the interaction between a given excitatory and inhibitory input by effectively changing the shunting character of inhibition. Effects of this type should be minimal for γ and δ cells compared with α and β cells because of their lower firing rate and the smaller charge factor (see §§3.1.7 and 4.1).

3.2.3. *Timing of excitation and inhibition*

When transient inputs are considered, the effectiveness of inhibition depends on the timing of the excitatory and inhibitory conductance changes. In general, one expects maximal effectiveness when the inhibitory conductance change overlaps maximally with the voltage change induced by excitation at the inhibitory location. For branched neurons and non-adjacent inputs approximate calculations of this type can be done with use of the formalism developed by Torre & Poggio (1978, 1981). Another possibility is to solve directly the system of Volterra integral equations. Even for adjacent inputs the inhibitory conductance change should be slightly delayed with respect to the excitatory conductance change (I. Segev, personal communication; Poggio & Torre 1978, 1981). Interestingly, for adjacent locations the optimal delay is very small (of the order of 5 % of the membrane time constant); this is

especially so for distal synapses on fine dendrites because their impulse response $K_{ij}(t)$ is usually quite fast. Our main results are valid also for short transient inputs. Although the peak voltage in the soma can be approximated by using equations (2.15)–(2.18) with the corresponding K^{eff}, its time course depends strongly on the timing and location of the two inputs. A detailed study of the temporal properties of these nonlinear interactions and of their possible role in information processing will be presented elsewhere (Koch *et al.* 1982).

TABLE 6. VALUES OF K_{ij} FOR THE α CELL OF FIGURE 2, FOR SOME VALUES OF R_i AND R_m

(K_{ij} values for transient inputs (alpha function with $t_{\text{peak}} = 1$ ms) are given in parentheses.)

$\dfrac{R_m}{\Omega \text{ cm}^2}$	$\dfrac{R_i}{\Omega \text{ cm}}$	$\dfrac{C_m}{\mu\text{F cm}^{-2}}$	$\dfrac{K_{2,2}}{\text{M}\Omega}$	$\dfrac{K_{2,5}}{\text{M}\Omega}$	$\dfrac{K_{5,5}}{\text{M}\Omega}$
2500	70	2	42.2 (28.7)	3.2 (0.9)	5.7 (2.2)
2500	100	2	54.6 (43.0)	2.8 (1.2)	6.1 (3.3)
3000	70	2	44.3 (29.2)	4.0 (1.1)	6.6 (2.3)
8000	70	1	57.9 (37.7)	12.8 (3.1)	15.7 (4.2)

3.3. *Do these results depend on parameter values?*

We stress that the quantitative values computed for the various cells depend on the parameter values that are assumed. While our calculations are based on commonly observed values, the reasonable physiological range is relatively wide. By analogy with experimental estimates for the cat motoneuron and other cells (Barrett & Crill 1974*a*; Rall 1977), we have assumed, as explained in §2, the values $C_m = 2 \ \mu\text{F cm}^{-2}$, $R_i = 70 \ \Omega \text{ cm}$, $R_m = 2500 \ \Omega \text{ cm}^2$, and the condition of sealed dendritic terminals. Similar experimental values are not available for cat retinal ganglion cells. Values for C_m and R_i much different from these are not very likely. C_m does not affect in any case our steady state values. The resistivity of the somatic cytoplasm R_i is rather constant at about 70 Ω cm for several vertebrate neurons (see Barrett & Crill 1974*a*). It seems unlikely that R_i is lower than 50 Ω cm (see also Barrett 1975). Within this range of values our results would not be drastically affected (cf. table 2). For higher R_i, the 'on path' effect becomes more pronounced.

The range of R_m is much more uncertain. All of our conclusions, however, are not affected if $R_m < 5000 \ \Omega \text{ cm}^2$. Table 6, for instance, shows the case of $R_m = 3000 \ \Omega \text{ cm}^2$. A possible complication, suggested by Barrett & Crill (1974*a*; Barrett 1975) is that R_m may not be uniform over the neuron. One could envisage, perhaps, a high dendritic and a low somatic R_m (with $C_m = 2 \ \mu\text{F cm}^{-2}$). We have computed such an extreme case for the β_2 and the γ_2 cells. We have assumed for the β cell a dendritic $R_m = 8000 \ \Omega \text{ cm}^2$ and a somatic $R_m = 823 \ \Omega \text{ cm}^2$ (to obtain the same total membrane conductance $S/R_m^s + D/R_m^d$, as seen by an electrode in the soma). Our steady state values changed only slightly; the input resistance at the distal tips increased by 3 % and that in the soma increased by 4 %, whereas the transfer resistance from tips to soma increased typically by 9 % and that from dendrite to dendrite increased by 6 %. In the γ cell a dendritic $R_m = 8000 \ \Omega \text{ cm}^2$ and a somatic $R_m = 892 \ \Omega \text{ cm}^2$ yield a larger effect. Input resistance increases at the dendritic tips by 22 %, at the soma by 9 % and from tips to soma by 50 %. The subunit pattern changes only slightly, subunits becoming somewhat smaller. We have also computed the effect of these non-uniform values of R_m on the transient properties. For the β cell of figure 3 the soma input impedance function $\tilde{K}_{ss}(\omega)$ is essentially unaffected relative to

the uniform case; the transfer function $\tilde{K}_{1s}(\omega)$ from dendrites to soma is only very slightly altered from the case where $R_{\mathrm{m}} = 2500 \ \Omega \ \mathrm{cm}^2$ uniformly. Temporal properties are different for $C_{\mathrm{m}} = 1 \ \mu\mathrm{F} \ \mathrm{cm}^{-2}$, as is to be expected.

If, however, R_{m} had a uniformly very high value our results would be drastically affected. For $R_{\mathrm{m}} = 8000 \ \Omega \ \mathrm{cm}^2$ soma input resistances may increase by a factor of about 3, whereas terminal resistances may grow only by about 30 % (see table 6). As a result sizable subunits (for $c = 4$) would disappear almost completely in all ganglion cell types for d.c. inputs. For transient inputs however ($t_{\mathrm{peak}} = 1 \ \mathrm{ms}$) strong spatial inhomogeneities would remain under the same conditions. The subunit map for transient inputs then turns out to be very similar to figures 3–6. Thus, even for these extreme values of R_{m}, our analysis would be qualitatively applicable to the transient case. For d.c. inputs, however, the ganglion cells would be rather close to practical equipotentiality (within 25 % from extreme tips for the α cell).

Although the subunit map changes completely for $R_{\mathrm{m}} = 8000 \ \Omega \ \mathrm{cm}^2$, all the properties of inhibitory interactions (§2.3) remain valid. The main reason for this is that they depend more on the geometrical structure of the dendritic tree than on specific values of membrane parameters. In particular, R_{m} may be larger by orders of magnitude without affecting these conclusions. The F factor depends, however, on R_{i}: the main properties discussed above hold true for $R_{\mathrm{i}} > 30$–$50 \ \Omega \ \mathrm{cm}$. $R_{\mathrm{i}} = 50 \ \Omega \ \mathrm{cm}$ is considered to be the minimal reasonable value (Barrett 1975). In summary, whereas the concept of subunit is not valid for $R_{\mathrm{m}} = 8000 \ \Omega \ \mathrm{cm}^2$, it seems fair to say that our other results especially concerning inhibitory interactions are rather invariant to parameter values, within the general physiological range ($50 \ \Omega \ \mathrm{cm} < R_{\mathrm{i}} < 100 \ \Omega \ \mathrm{cm}$; $1000 \ \Omega \ \mathrm{cm}^2 < R_{\mathrm{m}} < 15000 \ \Omega \ \mathrm{cm}^2$). Our evaluation of the significance of the dendritic branching of the different types of ganglion cells depends, however, on the assumption that all ganglion cells of the different classes have the same values for their membrane parameters. Diameters of branches have also a similarly critical role and their estimation is unfortunately subject to the uncertainties of the staining method. For instance, much larger branch diameters in the γ and δ cells than the values indicated by our histological material may drastically lower the strength of the interaction (F).

Since all our results are based on data obtained by light microscopy we do not have direct information on the location of excitatory and inhibitory synapses. Recent data (Stevens *et al.* 1980*a*, *b*), however, suggest that, especially for α and β cells, most synaptic contacts are restricted to the plane of branching of the dendritic tree.

Finally, it is worthwhile to stress again that our results would be drastically affected if the dendritic membrane of some or all ganglion cells had significant active properties, although several conclusions may still remain valid.

4. FUNCTION AND ARCHITECTURE OF CAT RETINAL GANGLION CELLS

4.1. *Physiological dichotomies*

Three main dichotomizing subdivisions of retinal ganglion cells in the cat have been developed in recent years on the basis of their physiological properties. Here we relate our analysis of the electrical properties of the different morphological classes of ganglion cells, derived in the previous chapter, to their physiological properties.

(a) *Sustained–transient (or tonic–phasic) dichotomy*

Cleland *et al.* (1971) found that under appropriate conditions the time course of discharge following the onset or offset of a spot stimulus in the centre differed in X and Y cells, that of X cells decaying less rapidly. These different time courses of response led to the sustained versus transient dichotomy for concentric units. Our analysis suggests that a transient (bandpass) response cannot readily be related to passive electrical properties. Transient behaviour may result from active properties of the dendritic membrane or, more likely, from synaptic properties in the inner plexiform layer. It seems impossible to distinguish between a transient and a sustained unit on the basis of the passive electrical properties derived from the morphology of the cells.

(b) *Brisk–sluggish dichotomy*

The brisk–sluggish dichotomy is mainly based on the responsiveness of cells (Cleland & Levick 1974a). Brisk cells, commonly identified with α and β cells, have a responsiveness (i.e. firing frequency) that grows briskly with strength of stimulus (at its onset), whereas the response of sluggish cells increases far less steeply with stimulus strength and remains relatively weak under all conditions. The brisk–sluggish dichotomy may be related to the electrical properties of the various cells. The higher effectiveness of synaptic inputs in α and β cells together with their potentially larger number and spread could well underly at least part of the brisk–sluggish classification. There may be several other, not mutually exclusive reasons for the different responsivenesses of ganglion cells (cf. Lennie 1980).

(c) *Linear–nonlinear dichotomy*

The first clear distinction to be made among ganglion cells with concentrically organized receptive field is due to Enroth-Cugell & Robson (1966) and it is usually stated in terms of a linear–nonlinear dichotomy, X cells showing linear and Y cells nonlinear spatial summation over the receptive field.

Linearity, as usually meant for X cells, does not imply that the cell response is linearly related to input strength (for instance stimulus contrast); it means that an X cell responds in a spatially homogeneous way over the whole receptive field, linearly summating excitation and inhibition. Thus, a β cell, despite some nonlinear addition of conductance inputs common in all synapses, would be expected to show X type linearity in terms of its passive electrical properties. There is some evidence that the centre-surround organization of X-like ganglion cells in the turtle retina is generated in bipolar cells at the level of the outer plexiform layer (Marchiafava & Weiler 1980). The properties of X cells would then reflect linear summation of excitation and inhibition by bipolar cells via 'linear' synaptic transduction. In terms of our approach to synaptic interactions (§2.3.2) linear summation of excitation and inhibition requires that the excitatory equilibrium potential E_e and the inhibitory equilibrium potential E_i are, respectively, well above and well below the resting potential, a situation that is characteristic of most bipolar cells (Richter & Simon 1975). The nonlinear behaviour of Y cells can probably be accounted for by nonlinear regions, with a size roughly corresponding to the centres of neighbouring X cells, distributed throughout the receptive field (Hochstein & Shapley 1976a, b). Convergence of excitatory and corresponding inhibitory inputs of the

shunting type ($E_i \approx 0$) on each of the electrical subunits of an α cell (see figure 2) could give rise to strong nonlinear interactions within each subunit. As a consequence it would be impossible to find a null position for a one dimensional grating, i.e. a position such that the exchange with a uniform field evokes no response. This is the classical test to distinguish X cells from Y cells (Enroth-Cugell & Robson 1966). In this scheme the nonlinearity of Y cells would be post-synaptic, though restricted to small subunits of the receptive field. The essential requirement is that the subunit of the α ganglion cells should have two distinct equilibrium potentials, one for excitation and the other, near the resting potential, for shunting inhibition (cf. Marchiafava & Weiler 1980).

Nonlinearities located presynaptically to the ganglion cells clearly represent another class of possible models. Hochstein & Shapley (1976 b), in particular, have suggested a population of rectifying subunits distributed throughout, and superimposed on, the classical concentric receptive field. According to their model the rectifying property originates in the rectifying transduction of synapses in the inner plexiform layer of the retina. In any case it is quite suggestive that our analysis of passive electrical properties reveals that α but not β cells are spatially inhomogeneous and have electrically decoupled subunits roughly of the size of a β cell at the same eccentricity. Thus, we think that the electrical subunits shown in figure 2 may correspond in their size and location to the functional subunits of Hochstein & Shapley.

4.2. Functional properties of γ-like and δ-like cells

The morphological classes of α and β cells have been convincingly linked with the physiologically defined Y and X cell, respectively. The γ and δ cells should, by exclusion, the counterpart of what physiologists have come to call W-cells, that is non-X and non-Y (Stone & Fukuda 1974). The sluggish concentric cells of Cleland & Levick (1974 a), as well as the cells with unusual spatial organization (Cleland & Levick 1974 b), are W cells. Among the latter subclass Cleland & Levick described a variety of neurons called ON–OFF cells, local edge detectors, colour-coded cells, uniformity detectors and directionally selective cells. Almost all those non-concentric cells, despite their heterogeneous properties, seem in our opinion to have strong nonlinear characteristics, actually stronger than Y cells. Their response, for instance, cannot be predicted even approximately from a knowledge of the receptive field measured with a single spot stimulus (Cleland & Levick 1974 b). Their spatial resolution, in particular, is often much better than the size of the centre would suggest (under the hypothesis of linearity). Their surround is of the silent type, suggestive of a shunting, strongly nonlinear type of inhibition; instead of subtracting from the cells' activity it seems to veto the effect of simultaneous excitatory inputs. Some of their properties suggest the existence of several subunits within the receptive field, each performing a strongly nonlinear addition. In terms of our analysis the γ cells may fit well these nonlinear properties.

4.2.1. Information processing properties

Our analysis shows that γ and δ cells may have strong nonlinear interactions between excitation and inhibition of the shunting type. For conductance changes larger than 10^{-8} to 10^{-7} S, inhibition on the direct path is much more effective than in any other location. A critical feature is the almost complete ineffectiveness of inhibition located distal to excitation.

These properties of synaptic interactions coupled with the morphology of the branching

pattern of γ and δ cells suggest that each class may perform characteristic operations on the synaptic inputs (cf. Barlow & Levick 1965). Figure 8a represents an idealized dendrite of a γ cell without any branching, receiving excitatory and inhibitory synapses distributed from the tip to the soma. Our results imply that a given excitatory input will be effectively vetoed by
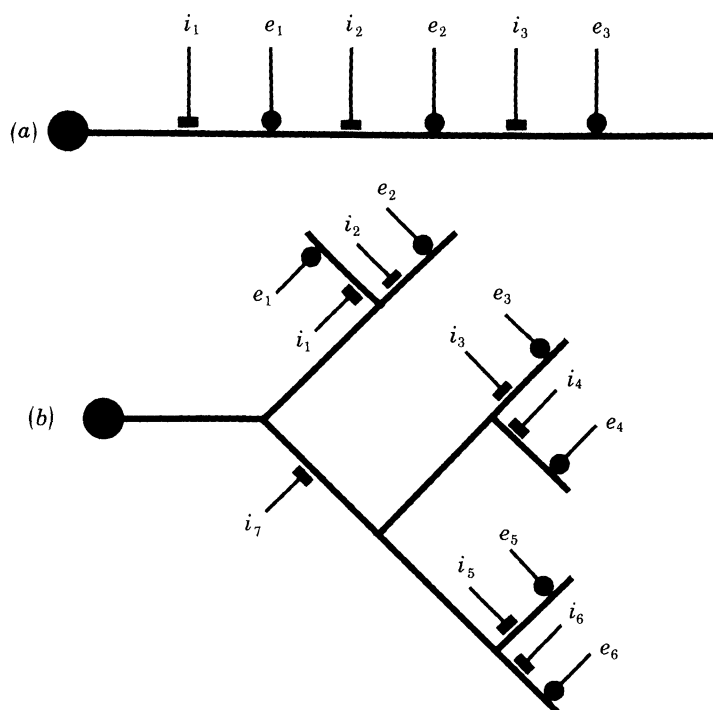

FIGURE 8. (a) An (idealized) dendrite of a γ cell receiving excitatory inputs ($\bullet$) and inhibitory inputs of the shunting type ($\blacksquare$). Any inhibitory input can effectively veto only more distal excitations and does not affect other inputs more proximal to the soma (compare table 4 and text). If the inhibitory interaction is described as an AND NOT gate the operation implemented in the figure could be read as

$$[e_3 \text{ AND NOT } (i_1 \text{ OR } i_2 \text{ OR } i_3)]$$
$$\text{OR } [e_2 \text{ AND NOT } (i_1 \text{ OR } i_2) \text{ OR } (e_1 \text{ AND NOT } i_1)].$$

(b) An (idealized) dendrite of a δ cell with excitatory and inhibitory synapses of the shunting type. Each inhibitory input i_1–i_6 vetoes specifically only the corresponding excitation (e_1–e_6), because it satisfies the appropriate direct path condition. Input i_7 can veto only e_3–e_6 for the same reason. Effectiveness of distant inputs such as i_7 is decreased by making smaller the excitatory conductance inputs (see table 5). The operation implemented in the figure would be logically of the type

$$(e_1 \text{ AND NOT } i_1) \text{ OR } (e_2 \text{ AND NOT } i_2) \text{ OR } \{[(e_3 \text{ AND NOT } i_3) \text{ OR }$$
$$(e_4 \text{ AND NOT } i_4) \text{ OR } (e_5 \text{ AND NOT } i_5) \text{ OR } (e_6 \text{ AND NOT } i_6)] \text{ AND NOT } i_7\}.$$

The inhibitory inputs i_1–i_6 must be relatively distant (more than 20–30 μm) from their branch point in order to leave unaffected the other excitatory inputs.

the inhibitory inputs on the direct path to the soma while remaining essentially unaffected by all other more distal inhibitory synapses. Clearly only certain logical patterns of operations can be performed on this basis.

A δ cell dendrite with its highly branched pattern can underlie a wider class of operations. An idealized δ cell dendrite with distal excitatory inputs and corresponding inhibitory synapses is shown in figure 8b. Each inhibitory input i_1 to i_6 vetoes specifically only the corresponding

excitation and affects only slightly the other excitatory inputs. Inhibition on one of the main branches, e.g. at i_7, can veto all excitatory inputs more distal to it on the direct path. For the sake of simplicity let us describe these interactions in terms of logical operations, bearing in mind that they are clearly much more complex than that. In these terms a conductance increasing shunting inhibition, respecting the 'on path condition', can implement an approximation of an AND NOT gate, whereas inhibition with an equilibrium potential more negative than the resting potential behaves similarly to an additive OR, especially if it is not located on the direct path of the excitatory input(s). The branched structure of the δ type with suitable synaptic inputs can thus perform sophisticated operations, based on an analogue nonlinear interaction of the logical type AND NOT. Direction selectivity, discussed in the next section, is just one example of the complex operations that could be performed by this simple mechanism (cf. Barlow & Levick 1965).

These ideas may be easily extended to show that a wide range of primitive nonlinear operations could be implemented by passive interactions between synaptic inputs. For instance, an approximation to the operation AND can be implemented by an excitatory input and another input decreasing the conductance to an ionic species with an equilibrium potential near the resting potential (located on the direct path to the soma). Local circuits mediated by synapses in both directions between dendrites of two or more neurons are sufficient to endow the simple AND NOT mechanism with the capability of implementing the analogue equivalent of all 'logical' operations. A full discussion should take into consideration several complex aspects of this general hypothesis. For instance interactions between transient inputs require a careful analysis; the analogue character of the interactions must be taken into account from the information processing point of view; and active membrane properties must also be included. In any case, the example of the γ and δ cells illustrate the fascinating aspects of this scheme, which is simply based on shunting inhibition and the branching geometry of the neuron. The central question is whether and to what extent the nervous system makes use of simple synaptic interactions of this type for processing information. There is little doubt that the conjecture about movement detection represents a critical test for these ideas.

4.3. Directionally selective cells: a conjecture

As described by several authors, and especially by Cleland & Levick (1974b), directionally selective cells in the cat have a low maintained discharge and rather circular receptive fields. They are selective for the direction of motion of a target passing through the centre. Movement in the opposite direction elicits no response, except at very low stimulus speed. Preferred and null directions are not predictable from a map of the receptive field. In addition, gratings with frequencies up to 3 cycles per degree can be resolved by the receptive field centre, although its diameter averages about 1°. Directional selectivity is usually independent of contrast although Stone & Fukuda (1974) found some ON directionally selective cells. Directionally selective cells in the rabbit retina are quite similar to the cat's; the latter are, however, less frequent and smaller. More important for us is that the underlying mechanisms may also be the same although the critical two-spots experiments (Barlow & Levick 1965) have not yet been done in the cat.

Two of us have recently proposed (Torre & Poggio 1978; see also Torre & Poggio 1981) specific synaptic interactions at the level of the ganglion cell dendrites as the mechanism underlying directional selectivity to motion. In this scheme, which extends the original proposal by Barlow & Levick (1965; see also Reichardt 1957), direction selectivity of ganglion cells is

based upon a multiplication-like inhibitory interaction between pairs of input regions. For motion in the null direction excitatory inputs are vetoed by inhibitory inputs of the shunting type originating from adjacent regions of the visual field. Directional selectivity is achieved by asymmetric delay (and/or low pass properties) in the excitatory and inhibitory channels from the photoreceptors to the ganglion cell. As shown by Barlow & Levick (see also Wyatt & Daw 1975) the veto operation must take place within small independent subunits contained within the receptive field and extensively replicated. The novel feature of the Torre–Poggio proposal concerns the nature of the veto operation and its localization. Inhibition is assumed to veto excitation at the level of the ganglion cell membrane as an effect of the nonlinear interaction taking place between electrically adjacent excitatory and inhibitory conductance changes (see §2.3.2). It has been shown (for a lumped model) that such a mechanism could account for the observations of Barlow & Levick (1965). In a dendritic tree, this type of postsynaptic multiplication-like inhibition is critically dependent on the electrical closeness of excitatory and inhibitory synapses. This is consistent with the result of Barlow & Levick that the inter-action responsible for directional selectivity occurs better at small separations of the stimuli than at large separations (Barlow & Levick 1965, p. 486 and tbl. 3). Replication of this mechanism in regions of the dendritic field that are electrically decoupled can subserve directional selectivity of the cell over a large receptive field, again consistently with the physiological data. Since nonlinearity of interaction is an essential requirement of this scheme, Torre & Poggio suggested that the optimal location for excitation and inhibition is on distal fine dendrites.

We wish now to link these ideas about directional selectivity to our analysis of cat ganglion cells. In a previous section we have shown that inhibitory inputs can shunt effectively and specifically more distal excitatory inputs in all ganglion cells. Especially γ and δ cells turned out to be an ideal substratum for nonlinear specific postsynaptic inhibition. In the context of our conjecture, therefore, a subclass of either δ or γ cells seems to represent an almost ideal morphological counterpart of the class of directionally selective cells.

4.3.1. *Are the cat directionally selective cells γ-like or δ-like?*

It is natural to ask whether directionally selective cells are more likely to be like the γ or the δ cells studied in this paper (cf. figure 1). The electrical properties of both γ and δ cells suit well our mechanism for movement detection. There are, however, also clear differences between the two types of cells from the point of view of movement detection.

We consider now two basic schemes for movement detection reflecting the different 'logical' properties of γ and δ cells. Imagine that fast excitatory and slow (or delayed) inhibitory pathways project roughly topographically from the photoreceptors onto the ganglion cell dendrites. A moving stimulus in the receptive field will be represented at the level of the ganglion cell as a wave of excitation followed by inhibition. An idealized dendrite of a γ-like cell is shown in figure 9a. In this case all centripetal movements of a small stimulus will be preferred and all centrifugal movements will be effectively vetoed. This is a simple consequence of the 'logical' properties outlined in figure 8a. Thus a γ cell with an anisotropic dendritic tree (in a planar section of the retina the dendritic tree is asymmetric for inversion of the motion axis, from the preferred to the null direction) can be made directionally selective (for small patterns) by topographic fast excitation and slow inhibition of the shunting type. For a γ-like cell with isotropic dendritic tree, directional selectivity can be obtained, in the framework of a mechanism based on shunting inhibition, only by suitably differential (with respect to the direction of
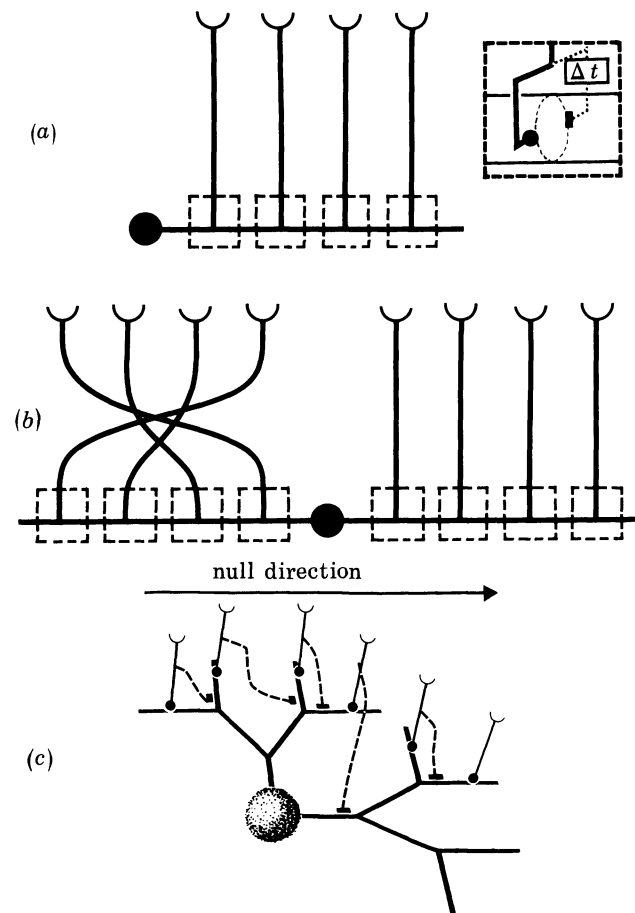
FIGURE 9. Three schemes for directional selectivity to motion, based on postsynaptic inhibition of the shunting type on a ganglion cell. Excitation (●) and inhibition (■) from the photoreceptors to the ganglion cell dendrites are carried through fast and slow pathway, respectively (see inset). Figure 9 (a) shows an idealized asymmetric γ cell with a dendritic tree that is not symmetric for inversion of the direction of motion. The null direction for a moving spot is centripetal, since proximal inhibition effectively blocks more distal excitation. Morphological asymmetries, as in figure 9 (a), can be substituted with asymmetries in the projection from the photoreceptors (figure 9 b). Such a γ cell may have a symmetric (with respect to the direction of movement) dendritic tree and be directionally selective. Figure 9 (c) shows, in perspective, a δ-like dendrite receiving topographic inputs from photoreceptors. The connections shown by broken lines represent slow (or delayed) inhibition. This scheme of movement detection can have a high grating resolution and small, compact subunits (see Barlow & Levick 1965). Its properties suggest that directionally selective cells may have a δ-like morphology.

motion) projections from the most distal retinal elements to the ganglion cells, as sketched in figure 9 b. Notice, however, that these schemes (figures 9 a, b) will perform much more poorly for movement of an extended pattern such as a grating with a spatial wavelength smaller than the diameter of the dendritic field, since long range inhibition effectively reduces the spatial resolution of directional selectivity (imagine a drifting, fine grating stimulating the γ cell dendrite of figure 9 a, b).

In a δ-like cell differential pairs of connections (i.e. with different delays or different low pass properties) seem the natural substratum for directional selectivity. The corresponding scheme is outlined in figure 9 c: each pathway produces a fast excitation on the distal part of a dendrite

which is vetoed for motion in the null direction by delayed inhibition at the base of the terminal branch. Direction sensitive interactions over a larger range can be simultaneously implemented by inhibitory inputs appropriately located at more proximal branches, which veto more than one excitatory input. Spatial resolution of direction selectivity (for instance for a grating) can be much finer than the size of the dendritic field (cf. Poggio & Reichardt 1976).

These three schemes for directional selectivity deserve several remarks:

(a) Some kind of anisotropy or asymmetry (i.e. differential distribution in space along the main axis of movement) of certain components is intrinsic to every scheme of directional selectivity (cf. Poggio & Reichardt 1976). In the first scheme (figure 9a) the morphology of the neuron itself is in this sense anisotropic. The second model (figure 9b) shows an asymmetry in the pattern of projections, but not in the dendritic tree. The asymmetry of the third scheme (figure 9c) lies in the arrangement of excitatory and inhibitory projections from the retina: each excitatory input is vetoed by slow inhibitory inputs from the null-direction side.

(b) In the first two models inhibitory inputs near the soma have long range effects, vetoing all distal excitatory inputs. In the δ cell scheme inhibition can be more localized in space. These properties can be immediately translated in terms of the notion of 'functional subunits', introduced by Barlow & Levick (1965). Two-spots (or slits) experiments may distinguish between the different possibilities. Directional selectivity for moving extended pattern can be much better in the δ-type model than in the other two schemes. In particular grating resolution may be quite poor in a γ cell, especially if the amplitude of the excitatory conductance change is relatively large.

(c) Various features of the idea proposed by Torre & Poggio (1978) are clarified by these models. In particular, we have shown the meaning of electrical 'adjacency' of excitation and inhibition for δ-like and γ-like cells. Furthermore, large F effects can be obtained in these dendritic trees also for excitatory inputs larger than inhibition, differently from the lumped circuit simulations.

(d) An alternative to the scheme of figure 9c, with several of the same attractive features, consists of presynaptic inhibition of the shunting type. Various lines of evidence, however, (see especially: Marchiafava 1979; Ariel & Daw 1982) support a postsynaptic mechanism of the type that we propose here.

Let us now return to the main question posed at the beginning of this section. Although more physiological data in the cat are clearly needed to allow a firm conclusion, we strongly favour δ-like cells as the morphological substratum for directional selectivity in the retina. This conjecture is based on three main points:

(i) Anisotropies in γ cell dendritic trees have not been reported yet and chiasma-like connections as shown in figure 9b seem somewhat unlikely. Thus the two possible schemes of directional selectivity for γ cells lack experimental support.

(ii) The properties of directionally selective subunits as reported by Barlow & Levick (1965) for the rabbit seem consistent with the δ cell scheme. The subunits are 'small compact ones' (about one-twelfth of the receptive field diameter or less), and in their number and coverage of the dendritic field area they readily correlate with the δ cell subunits of our model.

(iii) Directionally selective cells respond well to spatially extended patterns and not only to spots of light. In particular, their resolution for moving gratings is higher than the receptive field size would suggest (Barlow & Levick 1965; Cleland & Levick 1974b). The first two models

of figure 9 cannot account for this unless excitation is quite weak (then optimal inhibition is very near the location of excitation).

It is important to stress that our conjecture leaves relatively open the problem of the detailed circuitry needed for the temporal operations on the excitatory and inhibitory signals (for reviews about retinal circuitry see Boycott (1974) and Cervetto & Fuortes (1978)). An unequal delay or low pass operation could be performed in the inner plexiform layer by different kinetics of the excitatory and inhibitory conductances, possibly controlled by two different types of amacrine cells. The timing of the two inputs at the level of the ganglion cell is clearly critical for maximizing their nonlinear interaction. This issue will be examined in detail elsewhere.

One final point is worth mentioning: most (but not all) directionally selective ganglion cells in the retina of the cat are ON–OFF cells with a response that is independent of contrast reversal. In our scheme, this would require two kinds of subunits, the ones where OFF signals interact and the ones where ON signals interact. A bistratified (or diffuse) dendritic field in both the ON and the OFF layer would then become a very attractive design, although by no means necessary.

5. CONCLUSIONS

We summarize here the main results of our analysis for each of the four morphological classes of cat retinal ganglion cells.

(a) The α cells have a low input impedance and a large voltage attenuation from dendrites to soma. Their electrical properties are spatially inhomogeneous (if $R_m = 2500\ \Omega\ cm^2$). There are many subunits, electrically well decoupled. Each subunit is roughly of the size of a β cell at the same eccentricity. Higher R_m values would force the α cells towards a much greater equipotentiality. Within each subunit there may be moderate saturation effects on conductance inputs and possibly nonlinear interactions with inhibitory inputs; good linear summation between subunits is expected at the soma. Thus α cells are a likely basis for summation of independent input pools.

(b) The β cells at small eccentricities (e.g. 3 mm or less) have rather uniform electrical properties: distal and proximal inputs are roughly equivalent, voltage attenuation is low. Distal synapses have several properties of somatic inputs. Moderate nonlinear summation could take place as in α subunits. Thus, β cells are characterized by homogeneous spatial summation of their inputs, even distal ones. They are ideally suited to sum uniformly many inputs over the receptive field. At large eccentricity they become more inhomogeneous.

(c) Since γ cells are certainly a less homogeneous population than the previous two classes, we refer here to cells with a morphology as in figure 1. Cells of this type have a few subunits with high input impedance. As a consequence, γ cells could show a fair amount of nonlinear addition on single inputs, possibly underlying a sluggish character. Nonlinear interactions between distal excitatory and proximal inhibitory synapses on the direct path to the soma are very strong and specific, especially for shunting type inhibition; this holds true for normal as well as for very high R_m and R_i.

(d) The δ-like cells have a large number of subunits, which cover well the dendritic region. Within each subunit nonlinear interactions between distal excitation and proximal inhibition on the direct path to the soma are expected to be strong and isolated from other subunits.

Such a synaptic organization superimposed on the δ-like cell type of morphology seems ideal for underlying directional selectivity to motion.

REFERENCES

Ariel, M. & Daw, N. W. 1982 Pharmacological analysis of directionally sensitive rabbit retinal ganglion cells. *J. Physiol., Lond.* **324**, 161–185.

Barlow, H. B. & Levick, W. R. 1965 The mechanism of directionally selective units in rabbit's retina. *J. Physiol. Lond.* **178**, 477–504.

Barrett, J. N. 1975 Motoneuron dendrites: role in synaptic integration. *Fedn. Proc.* **34**, 1398–1407.

Barrett, J. N. & Crill, W. E. 1974*a* Specific membrane properties of cat motoneurones. *J. Physiol., Lond.* **239**, 301–324.

Barrett, J. N. & Crill, W. E. 1974*b* Influence of dendritic location and membrane properties on the effectiveness of synapses on cat motoneurones. *J. Physiol., Lond.* **239**, 325–345.

Baylor, D. A. & Fettiplace, R. 1979 Synaptic drive and impulse generation in ganglion cells of turtle retina. *J. Physiol., Lond.* **288**, 107–127.

Boycott, B. B. 1974 Aspects of the comparative anatomy and physiology of the vertebrate retina. In *Essays in the nervous system* (ed. R. Bellairs & E. G. Gray), pp. 233–257. Oxford: Clarendon Press.

Boycott, B. B., Peichl, L. & Wässle, H. 1978 Morphological types of horizontal cell in the retina of the domestic cat. *Proc. R. Soc. Lond.* B **203**, 229–245.

Boycott, B. B. & Wässle, H. 1974 The morphological types of ganglion cells of the domestic cat's retina. *J. Physiol., Lond.* **240**, 397–419.

Butz, E. G. & Cowan, J. D. 1974 Transient potentials in dendritic systems of arbitrary geometry. *Biophys. J.* **14**, 661–689.

Cervetto, L. & Fuortes, M. G. F. 1978 Excitation and interaction in the retina. *A. Rev. Biophys. Bioengng* **7**, 229–251.

Cleland, B. G., Dubin, M. W. & Levick, W. R. 1971 Sustained and transient neurones in the cat's retina and lateral geniculate nucleus. *J. Physiol., Lond.* **217**, 473–496.

Cleland, B. G. & Levick, W. R. 1974*a* Brisk and sluggish concentrically organized ganglion cells in the cat's retina. *J. Physiol., Lond.* **240**, 421–456.

Cleland, B. G. & Levick, W. R. 1974*b* Properties of rarely encountered types of ganglion cells in the cat's retina and an overall classification. *J. Physiol., Lond.* **240**, 457–492.

Enroth-Cugell, C. & Robson, J. G. 1966 The contrast sensitivity of retinal ganglion cells of the cat. *J. Physiol., Lond.* **187**, 517–552.

Famiglietti, E. V., Jr, Kaneko, A. & Tachibana, M. 1977 Neuronal architecture of On and Off pathways to ganglion cells in carp retina. *Science, N.Y.* **198**, 1267–1269.

Hartzell, H. C., Kuffler, S. W. & Yoshikami, D. 1976 The number of acetylcholine molecules in a quantum and the interaction between quanta at the subsynaptic membrane of the skeletal neuromuscular synapse. *Cold Spring Harbor Symp. quant. Biol.* **40**, 175–186.

Hochstein, S. & Shapley, R. M. 1976*a* Quantitative analysis of retinal ganglion cell classifications. *J. Physiol., Lond.* **262**, 237–264.

Hochstein, S. & Shapley, R. M. 1976*b* Linear and nonlinear spatial subunits in Y cat retinal ganglion cells. *J. Physiol., Lond.* **262**, 265–284.

Iansek, R. & Redman, S. J. 1973 The amplitude, time course and charge of unitary excitatory postsynaptic potentials evoked in spinal motoneurone dendrites. *J. Physiol., Lond.* **234**, 665–688.

Jack, J. J. B., Noble, D. & Tsien, R. W. 1975 *Electric current flow in excitable cells.* Oxford: Clarendon Press.

Koch, C. 1982 Nonlinear information processing in dendritic trees of arbitrary geometries. Ph.D. thesis, University of Tübingen.

Koch, C., Poggio, T. & Torre, V. 1982 Nonlinear interactions in a dendritic tree: localization, timing and role in information processing. (In preparation.)

Lennie, P. 1980 Parallel visual pathways: a review. *Vision Res.* **20**, 561–594.

Levick, W. R. 1975 Form and function of cat retinal ganglion cells. *Nature, Lond.* **254**, 659–662.

Marchiafava, P. L. 1979 The responses of retinal ganglion cells to stationary and moving visual stimuli. *Vision Res.* **19**, 1203–1211.

Marchiafava, P. L. & Torre, V. 1978 The responses of amacrine cells to light and intracellularly applied currents. *J. Physiol., Lond.* **276**, 83–102.

Marchiafava, P. L. & Weiler, R. 1980 Intracellular analysis and structural correlates of the organization of inputs to ganglion cells in the retina of the turtle. *Proc. R. Soc. Lond.* B **208**, 103–113.

Nelson, R., Famiglietti, E. V., Jr & Kolb, H. 1978 Intracellular staining reveals different levels of stratification for On- and Off-centre ganglion cells in cat retina. *J. Neurophysiol.* **41**, 472–483.

Peichl, L. & Wässle, H. 1979 Size, scatter and coverage of ganglion cell receptive field centres in the cat retina. *J. Physiol., Lond.* **291**, 117–141.

Peichl, L. & Wässle, H. 1981 Morphological identification of on- and off-centre brisk transient (Y) cells in the cat retina. *Proc. R. Soc. Lond.* B **212**, 139–156.

Poggio, T. & Reichardt, W. 1976 Visual control of orientation behaviour in the fly. II. *Q. Rev. Biophys.* **9** (3), 377–438.

Poggio, T. & Torre, V. 1978 A new approach to synaptic interaction. In Theoretical approaches to complex systems. *Lecture notes in biomathematics*, vol. 21 (ed. R. Heim & G. Palm), pp. 89–115. Berlin, Heidelberg and New York: Springer-Verlag.

Poggio, T. & Torre, V. 1981 A theory of synaptic interactions. In *Theoretical approaches in neurobiology* (ed. W. Reichardt & T. Poggio), pp. 28–38. Cambridge, Massachusetts: M.I.T. Press.

Poggio, T. & Torre, V. 1982 Biophysics of information processing. (In preparation.)

Rall, W. 1962 Electrophysiology of a dendritic neuron model. *Biophys. J.* **2** (suppl.), 145–167.

Rall, W. 1967 Distinguishing theoretical synaptic potentials computed for different soma–dendritic distributions of synaptic input. *J. Neurophysiol.* **30**, 1138–1168.

Rall, W. 1970 Cable properties of dendrites and effects of synaptic location. In *Excitatory synaptic mechanisms* (ed. P. Andersen & J. K. S. Jansen), pp. 175–187. Univ. forlaget Oslo.

Rall, W. 1977 Core conductor theory and cable properties of neurons. In *Handbook of physiology* (ed. E. Kandel & S. Geiger), pp. 39–97. Washington, D.C.: American Physiological Society.

Rall, W. & Rinzel, J. 1973 Branch input resistance and steady attenuation for input to one branch of a dendritic neuron model. *Biophys. J.* **13**, 648–688.

Redman, S. J. 1976 A quantitative approach to integrative function of dendrites. In *International Review of Physiology*, vol 10 (Neurophysiology II; ed. R. Porter), pp. 1–35. Baltimore: University Park Press.)

Reichardt, W. 1957 Autokorrelation-Auswertung als Funktionsprinzip des Zentralnervensystems. *Z. Naturf.* 12b, 448–457.

Richter, A. & Simon, E. J. 1975 Properties of centre-hyperpolarizing, red-sensitive bipolar cells in the turtle retina. *J. Physiol., Lond.* **248**, 317–334.

Rinzel, J. & Rall, W. 1974 Transient response in a dendritic neuron model for current injected at one branch. *Biophys. J.* **14**, 759–790.

Stevens, C. F. 1976 Molecular basis for postjunctional conductance increases induced by acetylcholine. *Cold Spring Harbor Symp. quant. Biol.* **40**, 169–173.

Stevens, J. K., Davis, T. L., Friedman, N. & Sterling, P. 1980a A systematic approach to reconstructing microcircuitry by electron microscopy of serial sections. *Brain Res. Rev.* **2**, 265–293.

Stevens, J. K., McGuire, B. & Sterling, P. 1980b Toward a functional architecture of the retina: serial reconstruction of adjacent ganglion cells. *Science, N.Y.* **207**, 317–319.

Stone, J. & Fukuda, Y. 1974 Properties of cat retinal ganglion cells: a comparison of W-cells with X- and Y-cells. *J. Neurophysiol.* **37**, 722–748.

Torre, V. & Poggio, T. 1978 A synaptic mechanism possibly underlying directional selectivity to motion. *Proc. R. Soc. Lond.* B **202**, 409–416.

Torre, V. & Poggio, T. 1981 An application: a synaptic mechanism possibly underlying motion detection. In *Theoretical approaches in neurobiology* (ed. W. Reichardt & T. Poggio), pp. 39–46. Cambridge, Massachusetts: M.I.T. Press.

Wässle, H., Boycott, B. B. & Illing, R.-B. 1981a Morphology and mosaic of On- and Off-β cells in the cat retina and some functional considerations. *Proc. R. Soc. Lond.* B **212**, 177–195.

Wässle, H., Illing, R.-B. & Peichl, L. 1979 Morphologische Klassen und zentrale Projektion von Ganglienzellen in der Retina der Katze. *Verh. dt. Zool. Ges.*, 1979, pp. 180–193.

Wässle, H., Peichl, L. & Boycott, B. B. 1981b Morphology and topography of on- and off-α cells in the cat retina. *Proc. R. Soc. Lond.* B **212**, 157–175.

Weiler, R. & Zettler, Z. 1979 The axon-bearing horizontal cells in the teleost retina are functional as well as structural units. *Vision Res.* **19**, 1261–1268.

Wyatt, H. J. & Daw, N. W. 1975 Directionally sensitive ganglion cells in the rabbit retina: specificity for stimulus direction, size, and speed. *J. Neurophysiol.* **38**, 613–626.